TEXAS Geosciences

The University of Texas at Austin

Jackson School of Geosciences

9th Annual

Jackson School of Geosciences

Student Research Symposium

February 15th, 2020

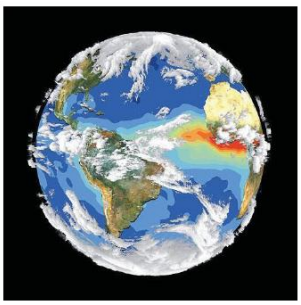


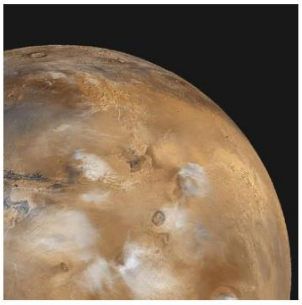

Welcome to the 9th Annual Jackson School Research Symposium!

It is with great pleasure we welcome you all to the 9th Annual Jackson School Research Symposium at UT-Austin! This symposium would not have been possible without the hard work of student volunteers, the support of faculty/research scientists, and generous support from ConocoPhillips. Thank you for taking part in supporting our students and growing research program within the Jackson School. Enjoy the posters!

This event is made possible with the support of

ConocoPhillips

Table of Contents

Themes:

Climate, Carbon, and Geobiology (CCG)

Energy Geosciences (EG)

Marine Geosciences (MG)

Planetary Sciences (PS)

Solid Earth and Tectonic Processes (SETP)

Surface Processes and Hydrology (SPH)

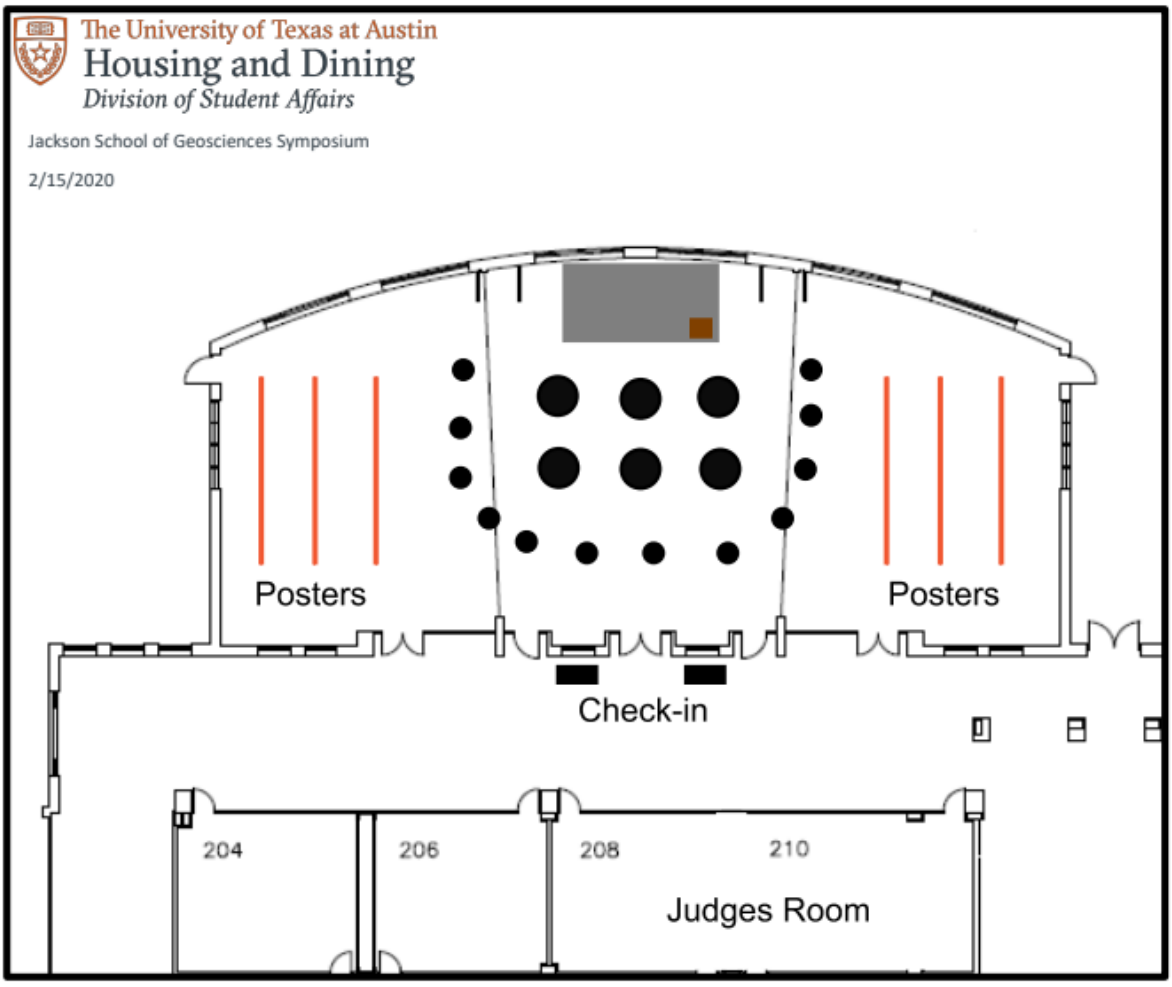

Schedule of Presentations and Events

Breakfast, A.M. session poster set-up.....8:30 a.m.
Early Career Graduate (ECG) posters.....9:00-11:30 a.m.
Late Career Masters (LCM) posters.....9:00-11:30 a.m.
Lunch, A.M. session poster take-down.....11:30 a.m.
P.M. session poster set-up.....12:30 p.m.
Undergraduate (U) posters.....1:00-3:30 p.m.
Late Career PhD (LCPHD) posters.....1:00-3:30 p.m.
Happy hour/judging.....3:30 p.m.
Awards/closing.....4:00 p.m.

Morning Session Posters

Early Career Graduate (ECG)	Poster #
John Moretti	ECG-1
Stacie Skwarcan	ECG-2
Yue Wu	ECG-3
Omar Alamoudi	ECG-4
Arnab Dhara	ECG-5
John Franey	ECG-6
Xin Liu	ECG-8
Landon Lockhart	ECG-9
Nam Pham	ECG-10
Bethany Rysak	ECG-11
David Wiggs	ECG-12
Yu-Chen Zheng	ECG-13
Zachary Murphy	ECG-14
Travis Stone	ECG-15
Emily Bamber	ECG-16
Kristian Chan	ECG-17
Eric Hiatt	ECG-18
Michelle Tebolt	ECG-19
Ethan Conrad	ECG-20
Erin Heilman	ECG-21
Nicholas Meszaros	ECG-22
Simone Puel	ECG-23
Daniel Ruiz Arriaga	ECG-24
Dimitri Voytan	ECG-25
Molly Zebker	ECG-26
Rawan Alasad	ECG-27
Evan Carnahan	ECG-28
Emily Carreno	ECG-29
Cansu Demir	ECG-30
Kwun Yip Fung	ECG-31
James Gearon	ECG-32
Scarlette Hsia	ECG-33
Ana Maria Restrepo Acevedo	ECG-34
Fernando Rey	ECG-35
Cole Speed	ECG-36

Late Career Masters Student (LCMS)	Poster #
Sinong Lin	LCMS-1
Esben Pedersen	LCMS-2
Ben Gremillion	LCMS-3
Nicole Guinn	LCMS-4
Samuel Robbins	LCMS-5
Hunter Manlove	LCMS-6
Micaela Pedrazas Hinojos	LCMS-7
Austin Rechner	LCMS-8

Afternoon Session Posters

Late Career PHD (LCPHD)	Poster #
Shuai Yan	LCPHD-1
Seungwon Chung	LCPHD-2
Sophie Goliber	LCPHD-3
Erin Keenan Early	LCPHD-4
Lingcheng Li	LCPHD-5
Natallia Piatrunia	LCPHD-6
Chijun Sun	LCPHD-7
Wen-Ying Wu	LCPHD-8
Ken Ikeda	LCPHD-9
Harpreet Kaur	LCPHD-10
Paul Morris	LCPHD-11
Son Phan	LCPHD-12
Qiqi Wang	LCPHD-13
Yuqian Gan	LCPHD-14
Dominik Kardell	LCPHD-15
Patrick Meazell	LCPHD-16
Eric Goldfarb	LCPHD-17
Naoma McCall	LCPHD-18
Megan Flansburg	LCPHD-19
Zachary Foster-Baril	LCPHD-20
Cullen Kortyna	LCPHD-21
Chelsea Mackaman-Lofland	LCPHD-22
Eirini Poulaki	LCPHD-23
Catherine Ross	LCPHD-24
Brandon Shuck	LCPHD-25
Wanying Wang	LCPHD-26
Evan Ramos	LCPHD-27
Logan Schmidt	LCPHD-28
Alison Tune	LCPHD-29
Logan West	LCPHD-30

Undergraduate (U)	Poster #
Lauren Lobue	U-1
Chinmay Murthy	U-2
Carole Lakrout	U-3
Thomas Quintero	U-4
Patricia Standring	U-5
Thomas Ditges	U-6
Anthony Edgington	U-7
Rachel Breunig	U-8
Ryan Herring	U-9
Xiafei Zhao	U-10

ECG

A Thick-billed Parrot (Rhynchopsitta pachyrhyncha) from Bonnell (LA 612) in Southeastern New Mexico and the Prehistoric Distribution of the Species in the American Southwest

John Moretti
Moretti, J., The University of Texas at Austin, Austin, TX

The archaeological site of Bonnell (LA 612) is significant as a Glencoe phase (A.D. 1200-1400) Jornada Mogollon settlement in the Sacramento Mountains of southeastern New Mexico. In a recent review of faunal remains recovered from the 1950s excavations, detailed comparative analysis demonstrates that an isolated tarsometatarsus represents *Rhynchopsitta pachyrhyncha*, the Thick-billed Parrot. Skeletal remains of Thick-bills, morphologically distinct from macaws, are known from 10 archaeological sites in Arizona and New Mexico. Thick-billed Parrots are specialist pinecone feeders that inhabit temperate mountain forests in the Sierra Madre Occidental of Mexico. A review of the archaeological occurrences illustrates that six sites, including Bonnell, are located within or nearby pine forest habitats suitable for Thick-billed Parrot ecology. Another three sites are situated within arid environments, but contain clear evidence of prehistoric cultural utilization of forest resources. This biogeographic distribution, combined with evidence from extant ecology, historic occurrences, and reintroductions, demonstrates an association between the archaeological sites and viable Thick-bill habitats. Southwestern archaeological Thick-billed Parrots, therefore, likely were procured within the region. This natural occurrence is in contrast to the cultural importation of Scarlet and Military Macaws into the Southwest. Accordingly, Thick-billed Parrots from Bonnell and other sites provide important evidence of the natural distribution of this presently endangered species.

Keywords: Thick-billed Parrot, Biogeography, Southwest archaeology, Holocene

CCG
ECG

Synthesis of paleoclimate, paleoecological, and archaeological data for central Texas over the last 20,000 years

Stacie Skwarcan
Skwarcan, S., University of Texas at Austin, Austin, TX

The Edwards Plateau in central Texas has been the subject of extensive paleoclimatic, paleoecological, and archaeological investigation since the mid-twentieth century, with the efforts of this work yielding over 700 publications. I am completing a compilation and synthesis of paleoclimate data relevant to the entire state of Texas and of paleoecological and archaeological data from the Edwards and Stockton plateaus that will provide a synthesis of the work that has been done regarding the climate, ecology, and human presence on the Edwards Plateau over the past 20,000 years. This type of compilation will aid in the identification of spatial or temporal gaps in knowledge where future work can be focused to answer questions including how humans, plants, and animals responded to past changes in climate from the late Pleistocene through the Holocene. Additionally, sites on the Edwards Plateau are uniquely positioned to record evidence of longitudinal shifts in the biogeographic and climatic boundary historically associated with the 100th Meridian, which has historically been recognized as a dividing line between the drier western United States and wetter eastern United States. If recent evidence of an eastward shift in that boundary is valid, and if an eastward shift continues, it may cause large population centers currently to the east of the boundary (e.g., Austin and San Antonio) to become more water-stressed. Determining whether and/or how this boundary has shifted in the past has the potential to aid in planning for future management challenges of water and other natural resources.

Keywords: Edwards Plateau, paleoclimate, paleoecology, archaeology, late Pleistocene, Holocene

CCG
ECG

Estimating soil organic carbon in the active layer of the Arctic Foothills using spaceborne InSAR surface deformation data

Yue Wu
Wu, Y., Aerospace Engineering, The University of Texas at Austin, Austin, TX
Chen, J., Aerospace Engineering, The University of Texas at Austin, Austin, TX
O'Connor, M., Jackson School of Geosiences, The University of Texas at Austin, Austin, TX
Ferencz, S., Jackson School of Geosiences, The University of Texas at Austin, Austin, TX
Cardenas, M., Jackson School of Geosiences, The University of Texas at Austin, Austin, TX
Kling, G., Ecology and Evolutionary Biology, University of Michigan, MI

Thawing permafrost can fuel large fluxes of carbon from land to the atmosphere, which may further accelerate global warming. Because the Arctic covers continent-sized areas that are mostly inaccessible, remote-sensing has become a critical tool for observing the continuous permafrost. Particularly, the density difference between liquid water and ice causes seasonal ground surface deformation that can be detected over large spatial scales using InSAR. We jointly analyzed the InSAR deformation signal from 12 ALOS PALSAR scenes and the hydraulic properties and stratigraphies of over 200 sites across the Arctic Footslope to determine what factors control seasonal freeze-thaw (FT)-related land surface deformation patterns. We discovered a strong relationship between the seasonal FT deformation signal, land vegetation cover types, and soil organic carbon content. Deformation amplitude increases along a geomorphic-ecohydrologic transect, with the smallest deformation occurring in heath vegetation on the drier ridge-tops, intermediate deformation in tussock-dominated hillslopes, and the largest deformation occurring in lowland valley-bottoms dominated by wet sedge. The strong agreement between the remote sensing and field measurements suggest that InSAR has greater observational capabilities than previously assumed for monitoring changes in hydrological and ecological characteristics above continuous permafrost.

Keywords: Soil Organic Carbon, InSAR, Active layer, Arctic Foothills

EG
ECG

Design and Initial Result from the X-ray Enable Tri-axial Testing Apparatus (X-RETTA)

Omar Alamoudi
Alamoudi, O., Jackson School of Geosciences, The University of Texas at Austin
Tisato, N., Jackson School of Geosciences, The University of Texas at Austin

Rocks with low porosity and permeability (tight rocks) have become a viable economic target in recent years. This is due to the economic feasibility of the production of their pore-filling hydrocarbons. It is now common to use techniques such as fracking to access and extract such pore fluids. Fracking involves perturbing the in-situ stress condition of subsurface rocks. The goal is the creation of new fractures or the activation of natural sealed fractures. These fractures become the conduit through which hydrocarbon fluids can flow.
Understanding how the introduction of these fractures affects the hydraulic permeability of these rocks is important geologically, and for the economics of a hydrocarbon system.
The most realistic way to understand how fracking affects hydraulic permeability requires testing rock samples in a laboratory. Samples are tested at pressures and temperatures that resemble in situ conditions (e.g., >10 MPa). Also, testing involves controlling other parameters such as differential stress or pore pressure. Such in-situ conditions are applied using tri-axial testing devices that limit visual inspection of the sample while testing.
Here we present the design and the initial results of a new X-Ray Enabled Tri-axial Testing Apparatus (X-RETTA) that can perform rock testing in a micro-CT. Testing was performed on synthetic material. Our samples are 25mm (1 inch) in diameter and 1:2 diameter to length ratio. For samples of this size, the X-RETTA is capable of approximately producing confining stresses and pore pressure of 20 MPa, and axial stress of 150 MPa. These applied stresses are continuously controlled and maintained, and are sufficient to reproduce the in-situ stress conditions that could fracture rock samples in an unconventional hydrocarbon play.
There are five unique features about the X-RETTA: 1) Samples are enclosed in an aluminum pressure vessel allowing for X-ray imaging of the sample during tri-axial testing; 2) top and bottom sample end-faces are independently probed by fluid pressure sensors that can be used in measuring the permeability of the samples continuously; 3) embedded piezoelectric sensors are used to passively monitor micro-cracking activity and measure P- and S-wave velocities; 4) the stress conditions are imposed using pressurized fluid circuits with integrated pressures sensors that allow for precise pressure control and continuous monitoring, and 5) the X-RETTA is capable of applying different strain rates.
Undergoing studies will focus on understanding the effect of strain-rate on the formation and propagation of fractures and hydraulic permeability of tight rocks. Two rock formations will be studied: the Eagle Ford shale and Buda Limestone. These two lithologies are chosen based on their availability, industry interest, and the wealth of literature addressing them.

Keywords: rock physics, fractures, microCT, triaxial testing, rock mechanics

EG
ECG

Multimodal reversible jump MCMC method for elastic and petrophysical seismic inversion

Arnab Dhara
Dhara, A., Jackson School of Geoscience

An emerging technology in geophysics is the stochastic inversion of geophysical data in order to estimate rock and fluid properties. Stochastic approaches allow sampling of multiple solutions of model parameters from their posterior distribution and quantifying uncertainty in the model parameter predictions. Here we propose a novel Amplitude variation with Offset (AVO) stochastic inversion algorithm to estimate elastic and petrophysical properties from prestack angle gathers. Our inversion algorithm uses a transdimensional bayesian inversion scheme. In this scheme, the number of model parameters (i.e. the number of layers) is treated as an unknown, and a reversible jump Markov Chain Monte Carlo (rjMCMC) algorithm is used to sample the model space. Our MCMC algorithm is also designed for the case of multimodal distributions of model parameters. The target model parameters for this inversion include categorical variables like facies and continuous elastic or petrophysical properties. The distribution of continuous properties is multimodal and non-parametric with the number of modes equal to the number of facies. Because of non-linearity of the forward model, the non-parametric nature of the distribution of model parameters and the large number of modes, an analytical solution to the bayesian problem is difficult to obtain. We use an MCMC method in which we iteratively sample the facies, by moving from one mode to another, and petrophysical properties, by sampling within the same mode. We demonstrate the efficacy of the algorithm on both synthetic and real data.

Keywords: AVO Inversion, MCMC statistics, Bayesian Inversion

EG
ECG

Interpretation of Miocene subbasins in the Wheeler domain

John Franey
Franey, J., Bureau of Economic Geology
Meckel, T., Bureay of Economic Geology

Carbon capture and storage (CCS) is currently one of the leading ideas to mitigate atmospheric emissions. To create a recognizable effect on the current atmosphere, megatonnes of carbon must be removed from the carbon cycle permanently. This requires a storage site that is both volumetrically massive and secure over geologic periods. The northern Gulf of Mexico has the ability to serve as a major location as a future site for carbon sequestering. Miocene deltaic systems are an ideal location for such work due to their proximity to the coast and carbon-producing refineries, high-quality sands, and depth relative to overpressure. The Corsair delta was a major sediment depositional center during the middle to upper Miocene and can fulfill the role as a potential site for carbon sequestration. The Corsair delta was active for approximately 10 million years (15.97-5.33 ma) and is located near the modern Matagorda Bay. Determining the spatial expanse of reservoirs is an important step in estimating the total volume of CO_2 that could potentially be injected. It is necessary to accurately map the extent of the deltaic system and understand how the system progrades, retrogrades, and aggrades throughout the Miocene. Detailed seismic mapping and seismic attribute generation will allow for interpretation of geomorphologic events that are both above and below seismic resolution.

The available seismic dataset that covers the Miocene corsair delta has a vertical resolution of approximately 75 feet. Many of the actual depositional features of the delta fall well below this threshold. Currently, this prevents accurately mapping the main sediment depositional centers of the delta as well as the transition zone from delta fringes to shoreface. This project will implement a dip-steering seismic volume to improve resolution and interpretation of these features. A dip-steered seismic volume records the azimuth and dip of seismic features at every point where inlines and crosslines intersect. From this seismic volume, seismic attributes such as similarity, curvature, and dip can be generated that will resolve features below conventional seismic resolution. Seismic dips generated from dip-steering can be tracked to inform on chronostratigraphic intervals. Well logs will be used to ground truth seismic interpretations and add lithographic information. Once the chronostratigraphic analysis is complete, the dataset can be transformed into a 3D Wheeler model. Transforming the seismic data into the Wheeler domain will flatten the chronostratigraphic events in 3D space. System tract interpretations (transgressive, highstand, falling stage, and lowstand) will be applied to the intervals.

An interpreted, 3D Wheeler model of the Corsair delta will improve interpretations of the spatial distribution of sands throughout the Miocene. Importantly, the model will highlight areas of non-deposition throughout the Corsair delta. These interpretations will aid in mapping potential CO_2 injection sites two-fold. First, the 3D Wheeler model can aid in risking future injection sites. Areas of high sand deposition can be spatially restricted according to the Wheeler model. Potential seals for injection reservoirs will correspond with condensed sections interpreted from system tracts. Finally, volume estimates can be made from the spatial extent of reservoir quality sand for future CCS projects.

Keywords: Carbon sequestration, Stratigraphic framework, Seismic attributes, Wheeler domain, Dip-steering

EG
ECG

Estimation of subsurface stress from seismic data: A feasibility analysis

Xin Liu
Liu, X., Institute of Geophysics
Sen, M., Institute of Geophysics

The processes that contribute to the in-situ stress field primarily include plate tectonic driving forces, gravitational loading and some human activities such as hydraulic fracturing and drilling. Plate driving forces cause the motions of the lithospheric plates that form the crust of the Earth. Gravitational loading forces include topographic loads and loads owing to lateral density contrasts and lithospheric buoyancy. These are modified by the local processes such as volcanism, earthquakes (fault slip), and salt diapirism. Human activities such as mining and fluid extraction or injection can also cause local stress changes. Because the largest components of the stress field (gravitational loading and plate driving stresses) act over large areas, stress orientations and magnitudes in the crust are remarkably uniform. However, local perturbations, both natural and manmade, are important for the application of geomechanical analyses for drilling and reservoir engineering decisions.
Geological effects can impact the design and successful completion of oil, gas, and geothermal wells. Understanding the stresses and pore pressures within the subsurface is important for the development of a geomechanical model that can guide well design as part of an integrated process to minimize cost and maximize safety.
Conventionally, Stress estimation is heavily dependent on wells, such as: leak off test; well logs and core data analysis, which only provide accurate information at some specific locations. However, if we want to know the stress state far away from the well, or before the well is drilled, the only available information is seismic data.
In this work, through a sensitivity test and seismic inversion for some simple models, I demonstrate the feasibility of estimating subsurface stress from seismic data. In order to build up a bridge between stress and seismic data, I propose a workflow, which consists of four steps. Step 1, initialize a stress model based on geomechanical modelling or geological information. Step 2, calculate anisotropy from the stress-stiffness relationship obtained from my previous work. Step 3, synthesize seismic data and compute the misfit between the observed data. Step 4, if the misfit is small or converged, output the stress state as the final stress, otherwise, go back to step 1 and update the stress model and repeat this workflow until the misfit converges.

Keywords: Subsurface stress estimation, seismic inversion

EG
ECG

Pressure Prediction in Unloaded (Unconventional) Basins. Case Study: Delaware Basin

Landon Lockhart
Lockhart, L., Department of Geological Sciences, The University of Texas at Austin, Austin, TX
Flemings, P., Institute of Geophysics and Department of Geological Sciences, The University of Texas at Austin, Austin, TX
Nikolinakou, M., Bureau of Economic Geology, The University of Texas at Austin, Austin, TX

I present a methodology to predict pore pressure in the eastern portion of the Delaware Basin that accounts for the 7,000 feet of erosional unloading that has occurred. In this location, pore pressure is approximately hydrostatic from the Delaware Mountain Group to the Bone Spring Formation (Fig. 1). Beneath the Bone Spring Formation, overpressures (u_e) reach an overpressure ratio ($\lambda^* = u_e/(\sigma_v-u_h)$) of 0.81, where σ_v is the vertical total stress, and u_h the hydrostatic pressure.
I couple two processes to predict pressure. First, I model the effects of unloading on the velocity-effective stress relationship using the approach described by Bowers (1995):

(Equation 1)

where v is velocity, v_0 is velocity at zero effective stress, σ'_v is the vertical effective stress, σ'_{max} is the maximum vertical effective stress to which the material has been subjected, U is a measure of the plasticity of the material, and a and b are lithology-dependent constants. I cross-plot velocity versus vertical effective stress in the hydrostatic interval and apply the following equation to shift the measured vertical effective stresses laterally to a point which corresponds to the "paleo" virgin curve (σ'_{vc}):

(Equation 2)

I compute σ'_{vc} assuming U=8 and calculate σ'_{max} given the current vertical effective stress plus the change in total vertical stress less the change in hydrostatic pressure ($\sigma'_v + \Delta\sigma_v - \Delta u_h$). I fit a power-law regression through velocity versus σ'_{vc} to obtain a and b in Eq 1.
Second, I consider the effect of unloading on the pore pressure through application of Skempton's pore pressure coefficient (B):

(Equation 3)

Pore pressure change due to undrained loading depends on the ratio of bulk (β) and fluid (β_f) compressibility. Equation 3 calculates the change in pore pressure that occurred due to unloading.
Finally, I combine the results from Equation 1 and Equation 3 and directly predict the present-day pore pressures. Lower values of B or U result in higher predicted pressures (Fig. 1). For the Delaware Basin, I find that a B=0.75 (Eq. 3) with an assumed unloading parameter U=8 (Eq. 1) predict pore pressures that most closely match the observed pressures. In future work, I will determine B from loading-unloading experiments in the laboratory, and estimate U from velocity measurements made during unloading.

Keywords: Pore pressure prediction, stress, strain, geomechanics, petrophysics

EG
ECG

Uncertainty in geophysical interpretation with deep learning

Nam Pham
Pham, N., Bureau of Economic Geology, The University of Texas at Austin, Austin, TX
Fomel, S., Bureau of Economic Geology, The University of Texas at Austin, Austin, TX

Uncertainty is an important aspect in geophysical interpretation. Using neural network with modified loss functions and dropout layer can help quantify the uncertainty of using deep learning for geophysical interepretation. The uncertainties include aletoric uncertainty (uncertainty related to noise in data) and epistemic uncertainty (uncertainty related to model parameter). With these uncertainties, geologists and interpreters can involve in the workflow of using machine learning for geophysical interpretation: how much we can trust the results from deep learning model and which way we can polish the results.

Keywords: geophysical interrpretation, uncertainty, neural network

EG
ECG

Analysis of Hydraulic Fracture Segmentation Features in the HFTS1 Slant Core: Wolfcamp Fm., Midland Basin, West Texas

Bethany Rysak
Rysak, B., Jackson School of Geosciences, The University of Texas at Austin, Austin, TX
Gale, J., Bureau of Economic Geology, The University of Texas at Austin, Austin, TX

The SCW slant core is part of the multidisciplinary Hydraulic Fracture Test Site project in the Midland Basin. The slant core made a close pass by two horizontal wells on an 11-well pad, and has yielded new insight into fracture networks created by the hydraulic fracturing process. Approximately 600 ft of core was recovered in six parts, through the Upper and Middle Wolfcamp. Fracture characterization identified 375 hydraulic fractures (trending E-W), along with 309 calcite-sealed natural fractures (Set 1 trending NE-SW; Set 2 trending WNW-ESE).

In this study, more in-depth analysis will be done focusing on the many shape and surface features of the hydraulic fractures, and their spatial distribution relative to each other and to the nearest completion stages in adjacent wells. From initial observations it can be seen that irregularly shaped hydraulic fractures tend to occur at the intervals closest to the stimulated wells. It has also been observed that the number of hydraulic fractures in core is potentially higher than the number of hydraulic fractures that we estimate to have initiated via completion processes. This observation may be tied closely to the many examples of twist-hackle segmentation and bifurcation seen in the core. These features can be used to determine propagation direction as well as build a clearer picture of fracture network growth and geometry. Interaction of hydraulic fractures with each other, with natural fractures, with concretions, and with changes in lithology directly impacts network complexity, and may influence proppant distribution.

The key implications of this work could provide a greater understanding of fracture network propagation in the subsurface, and could have wider applications for completion and production techniques in unconventional reservoirs.

Keywords: Twist-Hackles, Bifurcation, Fracture Propagation, Subsurface Fracture Networks, Unconventional Reservoirs

EG
ECG

Mudrock Velocity Anisotropy Based on History of the Full Strain Tensor

David Wiggs
Wiggs, D., The University of Texas at Austin, Austin, TX
Flemings, P., The University of Texas at Austin, Austin, TX
Spikes, K., The University of Texas at Austin, Austin, TX
Nikolinakou, M., Bureau of Economic Geology, Jackson School of Geosciences, The University of Texas at Austin, Austin, TX

We show a workflow for the prediction of elastic stiffnesses from the full strain tensor. The result is a full stiffness tensor prediction for each element within a geomechanical model. The workflow to determine elastic stiffnesses from the strain tensor requires four steps. Step one is to describe the principal strain tensor for each element in the model. The tensor is described from the outputs of a geomechanical model. Second, the principal strain tensor is used to describe porosity and aspect ratio with the assumption of incompressible grains. Third, properties for each constituent must be assigned. Fourth, the TI (transverse isotropy) stiffness matrix is computed relative to the axis of symmetry for each element. The necessary properties include the bulk modulus, κ, shear modulus, μ, and density, ρ for each constituent along with the volume fraction and aspect ratio of each inclusion. This workflow results in a cross-section populated with TI properties for each element generated from a geomechanical model. The results provide information about the impact of deformation on seismic imaging.

Keywords: Rock Physics, Seismic Anisotropy, Effective Medium Theory

EG
ECG

Oxygen-controlled ichnofabrics: Implications of the Oxygen-Level Recovery and Anoxic Events in the Austin Chalk Group, South Texas

Yu-Chen Zheng
Zheng, C., Bureau of Economic Geology; Department of Geological Sciences, The University of Texas at Austin, TX
Loucks, R., Bureau of Economic Geology, The University of Texas at Austin, TX
Ko, L., Bureau of Economic Geology, The University of Texas at Austin
Kerans, C., Bureau of Economic Geology; Department of Geological Sciences, The University of Texas at Austin, TX

The relationship between organic-rich, fine-grained sediments and benthic faunal activity as shown by analysis of trace fossil assemblages has been a subject of intensive research because of its utility for interpreting oxygen content of interstitial waters associated with source rock formations. Whereas the Upper Cretaceous Austin Chalk Group has been classically interpreted to be deposited in an oxygenated shelf sea, intervals of increased organic preservation in the Austin Chalk was recently ascribed to oxygen-deficient conditions in interstitial waters in South Texas. The evolution of benthic oxygenation conditions from oxygen-deficient to oxygenated during deposition of the Austin Chalk has not been well documented, nor has the paleoecological response corresponding to the variable and evolving sediment interstitial-water conditions. The continuous Gise #1 Core contained nearly the whole Austin Chalk section situated in Dimmit County provides an opportunity for detailed ichnologic and geochemical examinations. This study aims to integrate modern ichnologic and geochemical analyses to reconstruct paleo-oxygen history in the interstitial water in the Upper Cretaceous South Texas.
The results demonstrate that the Austin Chalk Group records the oxygen recovery of bottom water from anaerobic to aerobic conditions and punctuations of three anoxic pulses in the Upper Cretaceous of South Texas. Further, Ichnologic records concur with geochemical proxies illustrating this oxygen recovery history. The lowermost Austin Chalk consists of anaerobic (occasionally anoxic, in intervals contained trace elements enrichment) to dysaerobic sediments enriched in organic matter, transiting from more oxygen-deficient conditions of the underlying Eagle Ford Group. The bottom water was aerobic during the upper Lower Austin Chalk deposition, but three short-lived anoxic pulses punctuated within this interval. The middle Austin Chalk was deposited in a well-oxygenated, low-energy environment, characterized by slow and steady sediment accretion on the seafloor. Lastly, an increase in terrestrial composition, a slightly lowered oxygen content of the bottom water, and a reduced nutrient content in the environment in the Transition Zone produced depositional conditions similar to a slope environment characterized by the *Zoophycos* Ichnofacies.

Keywords: Austin Chalk, Ichnology, Benthic Oxygenation, Cretaceous, Anoxic Events

MG
ECG

Experimentally derived two-phase water relative permeability in the presence of methane hydrates

Zachary Murphy
Murphy, Z., Institute for Geophysics, The University of Texas at Austin, Austin, TX
Flemings, P., Institute for Geophysics, The University of Texas at Austin, Austin, TX
DiCarlo, D., Hildebrand Department of Petroleum and Geosystems Engineering, The University of Texas at Austin, Austin, TX

Methane hydrate reservoirs represent a significant portion of the global carbon cycle. In both geologic and production processes, multiple phases (gas, water, and hydrate) will be present in the reservoir. However, multiphase flow parameters are not well understood or documented in these systems. In order to model formation, flow, or production in hydrate systems, permeability and relative permeability are the most important parameters governing multiphase flow. In a drainage process, the non-wetting phase will first occupy the larger pores as the non-wetting phase saturation increases. The pore size distribution will control the relative permeability of both phases along a saturation path. To test this behavior in a hydrate system, we run steady-state relative permeability experiments at a range of hydrate saturations in a Berea Sandstone core. Two-phase relative permeability experiments are run in the same sample with and without hydrate. In a hydrate free sample, the wetting (water) phase relative permeability will decrease as the non-wetting (gas) phase saturation increases. In hydrate bearing samples, we observe that the relative permeability values of water at a given water saturation are nearly identical to the hydrate free sample. We interpret that hydrate acts as a non-wetting phase compared to the water and that hydrate will therefore preferentially form and exist in the larger pores. We observe that water relative permeability in the presence of methane hydrate can be modeled as a wetting phase relative permeability using a Brooks-Corey type model.

Keywords: hydrate, permeability, relative permeability, fluid flow

MG
ECG

Upper Triassic (Carnian) Sponge Reef Mounds from South Canyon, central Nevada.

Travis Stone
Bonuso, N., Department of Geological Sciences, California State University, Fullerton, Fullerton, CA
Stone, T., Jackson School of Geosciences, The University of Texas at Austin, Austin, TX
Williamson, K., California State University, Fullerton, Fullerton, CA
Agui, M., Department of Geological Sciences, California State University, Fullerton, Fullerton, CA

Critical reef evolution occurs in the Triassic Period. However, Upper Triassic reefs along the edge of the Panthalassa Ocean receive much less attention than their Tethys region counterpart. To help clarify reef evolution along the Panthalassa, we present a quantitative microfacies analysis to characterize reef facies types from a Central Nevada locality. We point counted thin sections to quantitatively access the relative abundance of reef and interstitial components from six Carnian reef mounds. Reef mound formation occurs at three different stratigraphic intervals. Each interval records a different reef mound size and shape. The oldest stratigraphic interval consists of four separate reef mounds; each mound is approximately 3-12 meters wide and 2-4 meters high. The second youngest stratigraphic interval consists of one large ~ 10-meter wide and 15.5-meter high domal reef mound. The third, and youngest, reef mound is smaller in comparison (i.e., 1-meter wide and 1.5-meter high). We recognize four reef facies types within these reef mounds. Different calcareous sponges, bound together by microproblematica such as *Tubiphytes*, and *Anisophytes*, and clotted micrite form the overall reef framework. We suspect that changes in relative sea level affect the initial colonization, different growth capacities, and overall preservation of the South Canyon reef mounds. Comparisons between other Carnian reef structures reveals that similar “Wetterstein-type” reefs persist within the Panthalassa region. Specifically, the South Canyon reef mounds closely resemble the SAC reefs – sponge dominated reefs comprised of bindstones.

Keywords: Triassic, Reef, Panthalassa, Sponge, Framework

PS
ECG

Sediment Transport and Aqueous Alteration in a Mars-Analog Glacial System.

Emily Bamber
Bamber, E., Department of Earth Sciences, University of Oxford, Oxford, UK
Rampe, E., NASA Johnson Space Centre, Texas, USA

Much of Earth's continental crust is felsic whereas Mars' upper crust is primarily basaltic. While we know much about both basaltic and felsic igneous materials, less is known about the weathering of basaltic terrains. An improved understanding of the products of alteration on basaltic terrains, across a range of climatic conditions, is therefore necessary for better interpretation of Martian mineralogy, especially given the geological evidence for a wide variety of aqueous alteration phases on Mars. This is even more pertinent given the apparent conundrum between climate models which can't reproduce an early Martian climate capable of sustaining liquid water, versus the geological evidence for channel incision, crater degradation, and aqueous alteration at a range of conditions.

During this internship project at the Johnson Space Centre, sediment samples from the valley of Collier glacier in the Three Sisters peaks, Oregon (OR) were examined. The underlying geology of this volcanic formation is dominantly basaltic andesite erupted within the last 50ka. Rapid retreat of the glaciers in the past few decades has allowed access to relatively fresh subglacial sediment for analyses. The young age of these moderately mafic igneous deposits and their recent exposure means that alteration by glaciers and meltwater should be the dominant factor in their alteration signal. Thus, the glacier valley sediments are considered an analogue to a possible "cold and icy" Mars.

The aim of the project was to better characterize erosion, transport, and in situ aqueous alteration in this modern terrestrial glacial system, with a view to compare results to observations of Mars. We examined the composition and morphology of different particle size fractions, from multiple sample locations across the Collier glacial valley, including of the bedrock. Samples were sieved and the %wt for each size-component was measured. X-ray diffraction (XRD) patterns were obtained for each particle size fraction and evaluated for compositional analyses. A more detailed analysis was conducted for a transect of moraine samples in the central glacial valley. Secondary electron images were obtained in an SEM for six samples to examine grain morphology.

We found that the mineralogical distribution across the glacial valley of Collier is influenced laterally by the distribution of distinct bedrock types on each side of the valley. Downstream, homogeneity increases while primary oxides and quartz become more confined to the finer-grained portions of a sample. The low abundance of any phyllosilicates or poorly-crystalline alteration confirms that glaciation of mafic terrains results in minimal chemical alteration, despite thousands of years of ice cover. While many of the features and mineralogical phases identified on Mars do not match our profile of a "cold and icy" basaltic terrain, the detection of amorphous phases on Mars may be consistent with cold/icy conditions. Additionally, given the weak alteration signatures produced by glacial terrains, it's possible this signal would be removed or masked by other periods of different alteration styles. Future work needs to better characterize how to uniquely identify ancient glacial terrains on Mars.

Keywords: Mars, analogue, XRD, glacial sediments

PS
ECG

Detection of Near-Surface Frozen Brines at Europa: Radar Investigation of a Canadian Arctic Analog

Kristian Chan
Chan, K., Institute for Geophysics, The University of Texas at Austin, Austin, TX
Rutishauser, A., Institute for Geophysics, The University of Texas at Austin, Austin, TX
Grima, C., Institute for Geophysics, The University of Texas at Austin, Austin, TX
Blankenship, D., Institute for Geophysics, The University of Texas at Austin, Austin, TX

Refrozen meltwater in porous snow and firn can serve as a terrestrial analog for hypothesized refrozen brines in Europa's porous ice regolith. Understanding near-surface (i.e. depth of meters to tens of meters) melt or brine mobilization on Europa is crucial for understanding shallow subsurface exchange mechanisms important to habitability of this icy moon. The Radar for Europa Assessment and Sounding: Ocean to Near-surface (REASON) instrument on the Europa Clipper mission is capable of detecting near-surface melt. Reflectometry measurements can be used to constrain the fate and evolution of melt through porous ice. We leverage Devon Ice Cap, Canadian Arctic, as a terrestrial analog to improve interpretation of radar signatures associated with percolated, refrozen meltwater in snow/firn.

The Radar Statistical Reconnaissance (RSR) method has been used to characterize terrestrial and planetary surfaces, by separating the coherent (specular) and incoherent (scattered) energy from radar returns. The incoherent component has been previously shown to correlate well with firn zones containing heterogeneous ice layers from refrozen surface melt. Here, we apply the RSR method to data collected over Devon Ice Cap with the University of Texas Institute for Geophysics High Capability Radar Sounder (HiCARS2). HiCARS2 is an airborne radar sounder operating at a 60 MHz center frequency and 15 MHz bandwidth (i.e. near-surface depth of 5 to 10 meters), similar to REASON. We compare the RSR results to firn cores and ground-penetrating radar data to understand the contribution of the near-surface structure (e.g. ice lens thickness and depth) to the coherent component. The coherent component is mainly sensitive to the permittivity, which can be related to the composition and deterministic structure of the reflecting interface. This study can augment the interpretation of radar sounding data for planetary exploration by detecting and characterizing near-surface environments with past melt/brine migration. It can also provide quantitative constraints on meltwater stored within the firn of ice masses affected by significant surface melt, which can benefit future surface mass balance studies.

Keywords: Europa, Brine, Radar

PS
ECG

The Dynamic Coupling Between Impact Induced Hydrothermal Activity and the Noachian Mars Hydrosphere: Implications for Habitability and Planetary Surface Processes

Eric Hiatt
Hiatt, E., University of Texas Institute of Geophysics, Jackson School of Geosciences, The University of Texas at Austin, Austin, TX
Hesse, M., Jackson School of Geosciences, The University of Texas at Austin, Austin, TX
Guilick, S., University of Texas Institute of Geophysics, Jackson School of Geosciences, The University of Texas at Austin, Austin, TX
Goudge, T., Jackson School of Geosciences, The University of Texas at Austin, Austin, TX

On Earth, plate tectonics has produced biologically favorable environments in hydrothermal systems associated with mid-ocean spreading centers where water, heat, and element cycling might have been conducive for the inception of life. In addition to mid-ocean ridges, impact-induced hydrothermal systems provide another setting to introduce sufficient energy for a biologically favorable environment. During the Late Heavy Bombardment, Mars experienced an impactor flux roughly 200 times the present rate. This is also a time when Mars had an active hydrosphere as indicated by geomorphic and spectral data**.** We are presenting the preliminary results for task one of a three-task project attempting to understand if impacts occurred at a spatiotemporal frequency sufficient to allow life to develop on Mars, and to persist by moving between impact-induced hydrothermal systems by groundwater flow.

Task one examines the scaling laws associated with impact basin formation and the time required for a hydrosphere to regain equilibrium. We developed a non-linear, numeric model based upon the Boussinesq approximation and built a Hele-Shaw cell to obtain experimental data that will be used to verify the model. By systematically altering the properties of the medium in the cell, we will be able to assess the model's accuracy across varying hydraulic conductivities. Task two will utilize these scaling laws to understand the time and extent materials will cycle through the hydrothermal system. Task three will be devoted to examining the conditions and time required to move material between adjacent hydrothermal systems.

Keywords: habitability, hydrology, planetary surface processes, post impact hydrothermal systems

PS
ECG

The Geometry of Fan Features on Mars

Michelle Tebolt
Tebolt, M., Jackson School of Geoscience, The University of Texas at Austin, Austin, TX
Goudge, T., Jackson School of Geoscience, The University of Texas at Austin, Austin, TX

Sedimentary rocks are extensively used on Earth as records of formative environments and regional climate at the time of deposition. Through the use of orbital data, similar observations and interpretations can be made regarding the sedimentary rocks on Mars. Martian sedimentary fan features are of particular interest because they can provide insight into the past hydrological cycle and climate of Mars. Previous studies have used the geomorphology of the fans to examine the depositional environment, but billions of years of erosion may have significantly altered the geomorphology of a fan deposit; however, the overall stratigraphy, or internal architecture, of a fan deposit will remain preserved. Here, we examine the stratigraphy of martian sedimentary fan features to constrain the reservoir(s) of liquid water associated with their formation. We consider two different fan features, one at the mouth of Tyras Vallis and another within Hargraves Crater, to evaluate if the depositional environment for each was subaerial or lacustrine. If the layers of the fan have relatively consistent dip from the mouth of the valley to the toe, this would be indicative of subaerial deposition in an alluvial fan. Alternatively, if the layer dips have slope breaks from shallow to steep and/or steep to shallow from the proximal to distal end of the fan, this is more indicative of a delta clinoform shape deposited into a standing lake. Taken together, our observations generally point towards a subaerial depositional environment for the Tyras fan, which has relatively shallow and consistent layers from proximal to distal end of the fan, and a deltaic depositional environment for the Hargraves fan where the slopes of the layers increase from proximal to distal end, which may be indicative of a slope break between topsets and foresets of a delta. Using fan stratigraphy to constrain the presence or absence of long standing bodies of water can help contribute to the understanding of the ancient climate of different regions on Mars at the time of deposition. For future work, we will conduct the same stratigraphic analysis on other fan features across Mars. The results will be used to constrain the size, location, and timing of water reservoirs across the martian surface.

Keywords: Mars, stratigraphy, deltas, alluvial fans

SETP
ECG

Plexiglass melt during rotary-shear experiments as an analog of pseudotachylite formation

Ethan Conrad
Conrad, E., Department of Geological Sciences, The University of Texas at Austin, Austin, TX
Tisato, N., Department of Geological Sciences, The University of Texas at Austin, Austin, TX
Cordonnier, B., Department of Geosciences and Physics, PGP, University of Oslo, Norway
De Siena, L., Institute of Geosciences, Johannes Gutenberg University, Mainz, Germany
Lavier, L., Department of Geological Sciences, The University of Texas at Austin, Austin, TX
Di Toro, G., School of Earth and Environmental Sciences, University of Manchester, Manchester, United Kingdom

The science of interacting surfaces in relative motion is known as tribology. Early studies outlined the governing principles such as Amonton's laws and the frictional Coulomb criterion. Further investigations include lubrication, healing and wear.
Tribology is applied to understand earthquakes including friction and energy dissipation in relation to fault strengthening and weakening mechanisms. In natural earthquakes the nucleation, propagation, termination and slipping velocity is the result of the accumulated and released energy around the seismic fault. Real time fault scarps are hard to monitor as they are usually at great depth, and under high pressure. Therefore, a more practical way to study earthquakes is in a closed laboratory setting.
Many tribological experiments use rotary shear tests. Rotary shear tests typically impose a predefined slipping velocity to materials in contact under a predefined load. Unfortunately, this conventional lab experiment has limitations compared to field scale earthquakes. This is because the lab failure occurs from an imposed velocity, whereas the field failure occurs from accumulated stress.
Here we present a unique rotary shear apparatus and experimental results that overcome some of the problems with conventional laboratory experiments. Our device implements a clock spring. When loaded by a motor, the clock spring imposes a linearly increasing torque to the sample. Such a set up allows simulated earthquakes to occur spontaneously when the shear stress on the slipping surface overcomes the normal load times the static friction. Therefore, the material surface interactions control when slip occurs, the velocity of slip and the total displacement. Furthermore, this method allows us to study both the precursory and co-seismic events that resemble those of natural slow-and fast-slip earthquakes.
We report the preliminary results of experiments with Poly(methyl methacrylate) (PMMA), commonly called plexiglass. PMMA is a transparent medium with a melting point of ~160°C and a glass transition temperature of ~105°C. PMMA's transparency allows us to observe the slipping surface at the contact between the two samples throughout the experiment. The experiments were recorded with a 60 fps video camera.
The experiment began with a spring loading rate of ~0.15 rpm. We observed frequent and seemingly "dry" low amplitude stick-slip events occurring at regular intervals. After this phase, we increased the rate to ~1 rpm. We then observed the formation and evolution of a melt film between the slipping surfaces. After each seismic event the melt layer solidified into a something similar to a pseudotachylite. This bonded the slipping surfaces. "Pseudotachylite" formation and surface bonding show fault strengthening, therefore leading to higher magnitude events. We also observed a particularly interesting phenomena during the transition period between the two loading rates, where possibly nanometer scale slip events resembled creep-like behavior.

Keywords: Friction, Earthquakes, Pseudotachylite, Fault strengthening

SETP
ECG

Visco-plastic, strain-dependent mantle convection modeling with deformation memory

Erin Heilman
Heilman, E., Institute for Geophysics, The University of Texas at Austin, Austin, TX
Becker, T., Institute for Geophysics, The University of Texas at Austin, Austin, TX

The efficiency of mantle convection and its surface expression, plate tectonics, depends on the Rayleigh number, rock rheology including plastic yield stress, and the heating mode. Previous models show Earth like plate dynamics, but the mechanisms behind yielding and the relationship between rock mechanics and models remain debated. Visco-plastic convection models show some of the hallmarks of plate, but there are a range of outstanding questions regarding the importance of inheritance and strain-localization. This motivates a range of efforts, including the use of “strain”, or damage, dependent yielding approximations to memory-dependent rheologies. Whenever strain-localization arises in convection models, numerical resolution must be evaluated as fine-scale features need to be resolved. On the other hand, certain formulations of visco-plasticity are inherently unstable and lead to mesh dependence. We therefore explore using the CIG community code *Aspect* for cylindrical visco-plastic convection computations with strain-dependence. We explore strain-dependent extensions and added strain-”healing” as well as a Frank-Kamenetskii approximation of temperature-dependence to the material model.

Keywords: Mantle convection, strain healing, ASPECT, modeling

SETP
ECG

Changing Volatile Contents Just Prior to Super-Eruptions: Evidence from the Upper Bandelier Tuff, Valles Caldera, New Mexico

Nicholas Meszaros
Meszaros, N., Department of Geological Sciences, Jackson School of Geosciences, The University of Texas at Austin
Nasholds, M., Earth and Environmental Science Department, New Mexico Institute of Mining and Technology
Gardner, J., Department of Geological Sciences, Jackson School of Geosciences, The University of Texas at Austin
Zimmerer, M., New Mexico Bureau of Geology and Mineral Resources

The existence of a partially molten magma reservoir under Valles Caldera raises the possibility of future catastrophic volcanic activity, thus prompting the need to determine the cause of the system's last VEI 7 eruption. Coincident with the timing of this major eruption was a petrologic shift in erupted high-silica rhyolites that is crucial in understanding the physical and chemical organization of the system. For ~360 kyr prior to the super-eruption, volcanism tapped two distinct magma batches: reduced fayalite-bearing rhyolite, and oxidized biotite-bearing rhyolite, both of which contain quartz and sanidine. The caldera-forming event only erupted reduced rhyolite, which has not erupted again in post-caldera volcanism. Here, we present volatile contents of quartz and fayalite-hosted melt inclusions and new high-precision sanidine $^{40}Ar/^{39}Ar$ ages to constrain changes in storage conditions for reduced rhyolites through the initial Plinian phase (Tsankawi Pumice) of the super-eruption. Preliminary $^{40}Ar/^{39}Ar$ ages indicate a hiatus of 3.5 ± 1.9 kyr between the last pre-caldera eruption (1235.3 ± 1.5 ka) and the start of the super-eruption (1231.8 ± 1.2 ka). Within this interval of several ka, CO_2 contents in quartz-hosted melt inclusions increased with statistical significance from 15 ± 34 ppm in pre-caldera tephras to 58 ± 48 ppm in the Tsankawi Pumice (Welch's t-test, $p << 0.05$). CO_2 was not detected in any fayalite-hosted inclusions, potentially due to post-entrapment leaking. Quartz-hosted melt inclusion H_2O contents between the Tsankawi Pumice and all pre-caldera tephras are similar, with a collective mean of 4.4 ± 1.4 wt.%, which is distinctly greater than the collective mean for fayalite-hosted inclusions of 2.8 ± 1.3 wt. % ($p << 0.05$). Estimated storage pressures from quartz-hosted inclusions range from 75-150 MPa for both pre-caldera eruptions and the super-eruption, which corresponds to storage at depths of ~3-5 km. In contrast to volatile compositions, major element compositions of quartz and fayalite-hosted melt inclusions are indistinguishable when corrected for post-entrapment crystallization of the host phase. The differences in volatile contents, but similarities in major element compositions, suggest that quartz and fayalite formed at different storage pressures from similar high silica rhyolite melts, only to be brought together immediately prior to eruption. Alternatively, quartz and fayalite may have formed at similar pressures, with fayalite-hosted melt inclusions being more prone to post-entrapment degassing than quartz-hosted inclusions. Similar CO_2 contents for tephra layers until the caldera-forming eruption suggests that the cause of the VEI 7 eruption was associated with an increase in magmatic CO_2 that occurred within 3.5 ± 1.9 kyr prior to the super-eruption. Rapid volatile content changes may thus be indicative of magma recharge that reorganized and destabilized the system prior to the Valles super-eruption.

Keywords: Valles Caldera, supervolcano, melt inclusions, magmatic volatiles, magma storage conditions

SETP
ECG

Application of FEniCS to Model Postseismic Deformations after Megathrust Earthquakes

Simone Puel
Puel, S., Department of Geological Sciences, The University of Texas at Austin, Austin, TX
Becker, T., Institute for Geophysics, The University of Texas at Austin, Austin, TX

Megathrust earthquakes are able to cause thousands of casualties and damage of billions of dollars. The major challenge to predict such events is due to the fact that we do not fully understand the processes which govern the stress build-up and how these stress perturbations are dissipated over time. Analysis of transient postseismic surface displacements, recorded by land-based and offshore GPS stations, may help to uncover the physics of these mechanisms occurring at depth. Among the three processes commonly used to explain surface deformation after a large earthquake (afterslip, poroelastic rebound and viscoelastic relaxation), the latter is thought to be the main mechanism able to explain longer time scale far-field GPS station behaviors. However, the estimation of viscosity of the Earth and how it changes over time remains uncertain and quite challenging. Advances in computational sciences may allow to build realistic physical models able to better infer the spatio-temporal evolution of such parameter. Here, we test the application of FEniCS, a free and open-source finite-element library able to solve PDEs, in order to model transient postseismic deformation after megathrust earthquakes. We test a new formulation of elasticity and viscoelasticity in which both displacement and stress are simultaneously calculated with the same accuracy. In addition, this approach allows a clean treatment of the fault discontinuity without adopting techniques such as split-nodes or introduction of non-cohesive cells to separate the relative motion of the two sides of the fault. We compare the results of the new approach with analytic solutions and the community software PyLith, which adopts the common displacement formulation. The building of a viscoleastic model represents the first step of an inversion framework which may be used to infer spatio-temporal variations in rheology after megathrust earthquakes, by directly inverting transient postseismic surface deformations recorded, for example, after the 2011 M9 Tohoku-oki earthquake.

Keywords: Earthquake modeling, subduction zones, computational science, geodynamics, postseismic deformation

SETP
ECG

FROM JURASSIC RIFTING TO CRETACEOUS-PALEOGENE INVERSION IN THE HUAYACOCOTLA AREA OF E MEXICO – INSIGHTS FROM STRUCTURAL GEOLOGY, GEO- AND THERMOCHRONOMETRY, AND STRATIGRAPHY

Daniel Ruiz Arriaga
Ruiz-Arriaga, D., Department of Geological Sciences, University of Texas at Austin
Stockli, D., Department of Geological Sciences, University of Texas at Austin
Fitz-Díaz, E., Universidad Nacional Autónoma de México

The Phanerozoic tectonic evolution of eastern Mexico is dominated by the complex interplay of subduction-related magmatism, back-arc extension, and retro-arc shortening as well as the opening of the Gulf of Mexico (GOM) during the break-up of Pangea. The major tectonic episodes that configured the E of Mexico include 1) the late Paleozoic tectonic assembly of Pangea, amalgamating granulitic Proterozoic Oaxaquian basement and early Paleozoic Gondwanan terranes, and associated Permo-Carboniferous arc magmatism. 2) Early Jurassic breakup of Pangea, opening of the GOM, incl. southward translation of the Yucatan block along the East Mexican transform, and formation of fault-bounded extensional basins. 3) Late Cretaceous–Paleogene shortening and associated foreland sedimentary successions associated with the Mexican Orogeny (MO). While early Mesozoic extensional basins exhibit thick fluvial to marine sedimentary successions, organic-rich shales, and evaporites, limited information is available for the syn-rift stratigraphy, facies distribution, provenance, basin thermal history or tectonic context in relation to GOM opening. This study presents new detrital zircon (DZ) U-Pb and (U-Th)/He provenance data integrated with sedimentologic and petrographic observations and regional stratigraphic correlations, to resolve the tectonic evolution from rifting to inversion in the Huayacocotla area, at west GOM. The DZ U-Pb data show that Permian Tuzancoa Fm. was deposited in an extensional basin exclusively sourced from the East Mexican Arc. Subsequent Jurassic syn-rift strata of the Huayacocotla and Cahuasas Fms. record unroofing of Oaxaquian basement and Permian arc and input of Jurassic arc magmatism, with sedimentary facies controlled by proximity to normal faults. Finally, Paleogene Chicontepec samples are characterized by Middle Jurassic and Cretaceous to Paleocene DZ ages derived from both the eroding Mesozoic strata in thin-skinned Mexican fold-and-thrusts belt and contemporaneous volcanism, but prior to inversion of the Jurassic rift basins. These preliminary data paint a clearer picture of late Paleozoic to early Cenozoic tectonic, magmatic, and basin evolution of east-central Mexico in response to Pangea assembly and break up and subsequent shortening and inversion during the MO.

Keywords: Gulf of Mexico, syn-rift, Huayacocotla, basin inversion, sediment provenance

SETP
ECG

Enhancing Tsunami Early Warning with Deep Learning

Dimitri Voytan
Voytan, D., University of Texas, Austin
Lay, T., University of California, Santa Cruz
Brodsky, E., University of California, Santa Cruz

Large thrust-faulting earthquakes on plate boundaries pose a significant tsunami threat, particularly if co-seismic fault slip extends up-dip to shallow depth on the megathrust. For a given earthquake magnitude, shallow slip significantly enhances tsunami excitation due to low rigity sediments in the wedge and increased seafloor displacement. Elastic waves generated from the rupture process that are incident on the seafloor convert to acoustic waves. It is convenient to think of these waves as exciting normal modes of the water column, where water depth controls the passband of the water reverberations. Numerical experiments and real data show that for earthquakes in deep water (> 3 km) settings, the acoustic reverberations are observed teleseismically at periods of ~7-15 s. The reverberations are easily identified as ringing in the P_{coda} and can thus be used to identify earthquakes with shallow slip in deep water and potential tsunami enhancement. For this discrimination task, we train a convolutional neural network (CNN) on vertical component velocity seismograms from 52 large ($M_w \geq 7.3$) megathrust earthquakes with known slip distributions to identify events as having shallow slip in deep water from events lacking shallow slip in deep water. We compare these results with simple time domain power measurements of the P_{coda} relative to P waves directly generated from the rupture process. The neural network approach performs comparably to the power measurement method with the advantage of not requiring *a priori* knowledge of the rupture duration. Events with shallow slip in deep water can be identified at epicentral distances <60° or ~14 min, which can supplement regional early tsunami warning.

Keywords: Earthquake Seismology, Tsunami, Deep Learning

SETP
ECG

Mapping the rate of carbon mineralization in Oman ophiolites from space

Molly Zebker
Zebker, M., The University of Texas at Austin
Chen, A., The University of Texas at Austin
Hesse, M., The University of Texas at Austin

Interferometric Synthetic Aperture Radar (InSAR) measurements reveal ground deformation related to rainfall, and subsequently carbonation, in the Samail Ophiolite in Oman. When the ophiolite is exposed to air and water, it undergoes carbonation which fractures the rock and mineralizes and permanently stores carbon, resulting in observable ground surface uplift. This process was previously thought to occur at a very slow rate and the mineralized carbon was thought to be 30-90 million years old. However, recent dating records reveal that the mineralized carbon is only 26,000 years old, thus the mineralization rate is much faster than initially estimated.

InSAR is a geodetic technique that uses the phase difference between two SAR images to measure a 2D map of surface deformation between two SAR acquisition times with mm-cm level accuracy, at 10s of meter spatial resolution, and near global spatial coverage. The resulting displacement map shows which areas have more uplift, due to carbonation, and the deformation rate can be calculated and interpreted in terms of carbonation.

A pilot study using 41 Sentinel-1 SAR images between 2016/11/15 and 2018/03/22 shows up to 4 cm of uplift in the several weeks following a major rainfall event, suggesting that carbonation is limited by rainfall. The uplift signal eventually recedes back to the noise level thus a longer time series with more rainfall events will better confirm this hypothesis. An eventual InSAR time series from 2015-present and an associated groundwater table model may improve the current estimates of CO_2 captured by carbonation, and its rate, in ultramafic rocks. These estimates influence ongoing research related to accelerating this process as a means to reduce our carbon footprint.

Keywords: InSAR, remote sensing, surface deformation, Oman Ophiolite

SHP
ECG

The Sedimentology of Early Rift Marine Flooding in The Gulf of California: Late Miocene Stratigraphy of the Fish Creek-Vallecito Basin

Rawan Alasad
Al-Asad, R., Jackson School of Geosciences, The University of Texas, Austin, TX
Steel, R., Jackson School of Geosciences, The University of Texas, Austin, TX
Olariu, C., Jackson School of Geosciences, The University of Texas, Austin, TX

In the Fish Creek-Vallecito Basin, 200 km north of Gulf of California, 500 m of alluvial fan conglomerates (Elephant Tree Fm.) are abruptly overlain by up to 60 m of evaporites (Fish Creek Gypsum), which are in turn overlain by marine turbidites of the Latrania Fm. This stratigraphic sequence suggests that during the opening of the Gulf of California the subaerial to subaqueous transition occurs rapidly without passing through a shallow marine phase. The purpose of this study is to: (1) understand the mechanism and sedimentologic response of the subaerial to subaqueous transition during the early stages of rift basin flooding, (2) understand the depositional setting and the common stratigraphic relationships between conglomerates, evaporites and turbidites in rift basins. Field work on the early syn-rift stratigraphy of the Fish Creek-Vallecito basin shows that: 1) the Elephant Tree Fm. deposits are basement-derived fault-controlled alluvial fans mainly comprised of dm to several meters thick matrix-supported conglomerate beds formed by subaerial debris flow processes, (2) the alluvial fans became flooded rapidly at a late stage and prior to the appearance of the evaporites. A subaqueous delta-facies association persists through the uppermost 30 m of fanglomerates and is comprised of cm to dm-scale normally graded beds deposited by high and low-density turbidity currents, (4) the occurrence of this subaqueous delta facies association is accompanied by a large rock avalanche mega-breccia facies suggesting that flooding occurred catastrophically due to tectonic instability, (3) these turbidites eventually interfinger with evaporites indicating that sediment-gravity flow processes alternated with subaqueous gypsum precipitation in deep hypersaline lakes that were isolated from open-marine environments. This stratigraphic sequence of alluvial fans to turbidites to evaporites is common in many other rift basins and can be thought of as the expression of proto-rift tectonics and earliest marine transgression. In the subsurface, the alluvial fans will be poor reservoirs because of the poor-sorting and likely low permeability, but the overlying turbidites will be better sorted, more aerially extensive tabular beds that will onlap onto alluvial fans and interfinger with evaporites forming sedimentary traps.

Keywords: Rift Basin, Alluvial Fans, Turbidites, Evaporites

SHP
ECG

Evolution of Greenland marine-terminating glacier dynamics throughout a 30-year period of stability and retreat

Evan Carnahan
Carnahan, E., Institute for Geophysics, University of Texas at Austin

Changes in mass resulting from evolving glacier dynamics are one of the largest contributors to recent mass loss from the Greenland Ice Sheet, yet individual glacier dynamic losses are highly variable even within a region. We examine the dynamics of the lower trunks of a group of glaciers in Greenland over a 30-year period where many, but not all, have gone from stable to retreating. Previous analysis of glacier dynamics has focused on individual time periods or single glaciers. By studying the evolving dynamic changes of several glaciers over an extended time period that includes significant mass loss, the controlling processes of dynamic mass loss are elucidated. A focus on these changes can validate previous theoretical work and provide better constrained predictions for future dynamic mass loss.

Changes in the dynamics of a glacier are understood through the balance of forces that are at play. Dynamic changes include variation in stress, strain, and velocity, which we calculate for individual glaciers from a variety of new freely available data products for the years from 1985 to 2015. The time-series of force balances allows us to examine the evolution of stresses during irreversible tidewater glacier retreat, and to compare this evolution across glacier catchments with differing dynamic responses to climate forcing. After calculating force balances between 1985 and 2015, we compare our findings to theoretical predictions for the transient evolution of stresses at play, and examine the accuracy of predictions for terminus stability.

Keywords: glacier, Greenland, inverse modeling, fluid dynamics, sea level rise

SHP
ECG

Using hydraulic modeling and high-resolution topographic data to predict river channel morphology during flood events.

Emily Carreno
Carreno, E., The University of Texas at Austin

Rivers are dynamic systems that respond to changes in discharge by adjusting themselves through processes of sediment transport. Large changes in discharge, such as flood events, are a natural occurrence for a river but provide a hazard for the many communities and large cities that are situated on the banks of rivers all around the world. The frequency and severity of flood events are increasing in many places due to anthropogenic climate change. As communities continue to exploit rivers for the many resources they provide, it will become increasingly important to know how rivers will evolve so that we can better manage them and mitigate risk. This study provides an opportunity to examine how well river morphodynamics can be predicted during flood events by using high-resolution topographic data and numerical modeling. Reaches in the Henry Mountains of southern Utah, and the Buëch River in southeast France will be involved in this study. Field work will be conducted at both sites to gather observational data as well as to execute UAV (Unmanned Aerial Vehicle) photogrammetry surveys. The new topography data will be used along with existing LiDAR data and several hydraulic modeling approaches to analyze how channel morphology varies during flood events and how well it can be predicted.

Keywords: geomorphology, morphodynamics, river, sediment, erosion, deposition, flood, modeling

SHP
ECG

The Mystery of Groundwater in Coastal Permafrost Areas. A Field Study: Kaktovik Lagoon, AK

Cansu Demir
Demir, C., Jackson School of Geosciences, The University of Texas at Austin, Austin, TX
Cardenas, M., Jackson School of Geosciences, The University of Texas at Austin, Austin, TX
Pedrazas, M., Jackson School of Geosciences, The University of Texas at Austin, Austin, TX
McClelland, J., Marine Science Institute, The University of Texas at Austin, Port Aransas, TX

Thawing permafrost due to climate change results in severe environmental consequences, such as impacting ecological processes and trajectories, accelerating nutrient and carbon cycling including the production and release of greenhouse gases, and modifying hydrologic flows and storage that impact connectivity between terrestrial, aquatic, and marine environments. In the case of the latter, groundwater plays an important role in the delivery of material to surface water bodies which include not only lakes, rivers, and wetlands but also coastal waters such as the lagoons lining the Beaufort Sea coast of Alaska. However, the groundwater flow regimes in seasonally thawed continuous coastal permafrost areas are still not well understood. Salinity and temperature, which are related by phase relationships at the ice-water boundaries, are vital parameters to comprehend the properties of subsea permafrost and the submarine groundwater discharge (SGD). In this study, we investigate the active layer (seasonally thawing/freezing) distribution, and saline-fresh groundwater mixing zone under Kaktovik Lagoon, one of the shallow lagoons surrounded by barrier islands in the Alaskan Beaufort Sea. This location is a good representative of the lagoon systems of the region. The field campaign includes measurements of hydraulic head, water salinity and temperature of the beach and lagoon substrate collected along a shore?perpendicular and –parallel transects at a sampling interval ranging between 1 m and 10 m horizontally, and 0.1 to 1 m vertically. This is done in conjunction with direct and indirect probing for the permafrost table, if it is present. We hypothesize that coastal lagoons have mostly thawed substrate reaching great depths. This implies that groundwater discharge and transport might be a prominent process. Furthermore, climate warming will enlarge the SGD pathways in the permafrost, and result in connected flow patterns which will result in higher organic loads to the lagoons. Our results have important implications for predicting the driving forces and quantifying the related fluxes of organic matter and gases between groundwater and lagoon in these environments. Our goal is not only to quantify these but also to improve the process understanding of groundwater flow and transport in Arctic lagoons.

Keywords: permafrost, groundwater, lagoon, salinity, temperature

SHP
ECG

Advance MODIS urban land use classification using Landsat images at Houston

Kwun Yip Fung
Fung, K., The University of Texas at Austin, Austin, TX
Yang, Z., The University of Texas at Austin, Austin, TX
Niyogi, D., Purdue University

Moderate Resolution Imaging Spectroradiometer (MODIS) land use land cover (LULC) product is one of the important product to describe the natural vegetation class and coverage since 2001. MODIS LULC product identifies global land surface into 17 classes defined by the IGBP scheme annually, including 11 natural vegetation classes, three human-altered classes (urban and built-up lands, croplands, and cropland/natural vegetation mosaics) and three non-vegetated classes with 500-m spatial resolution. MODIS LULC often supplies as the surface boundary condition for driving model simulation. However, to understand urban meteorology, a 500-m single type urban classification is too coarse. Therefore, this poster will describe how to advance the classification using 30-m Landsat images. This project will incorporate 10 different built-up local climate zones (LCZs) classification into the IGBP scheme. Landsat radiance data will feed as input. The radiance data are trained with the aid of Google Earth satellite images. Then, a random forest supervised classification is used to generate a 100-m LCZ map for Houston. Finally, the LCZ map is overlayed on the original MODIS LULC map.

Keywords: Landsat, WUDAPT, urban sprawl, local climate zones

SHP
ECG

Lacustrine Delta Architecture in the Ancient and Modern

James Gearon
Olariu, C., Department of Geological Sciences, The University of Texas at Austin, Austin, TX
Steel, R., Department of Geological Sciences, The University of Texas at Austin, Austin, TX

Lacustrine deltas call for careful interpretation as they are distinct from their marine counterparts. It has been recognized in previous publications that lacustrine delta-fronts are dominated by shallow, low-relief, sandy channels that drive sheet-sand deposition basin-ward. It is less discussed that lake base level can change meters over short time scales (100s of years) leading to high frequency progradational and retrogradational sequences which affect lake delta architecture. These "lake deltas" have distinct proximal-to-distal three-dimensional channel geometries which are recognizable in both the ancient (Middle Green River Fm.) and the modern (Neales Delta, Lake Eyre, Australia).
In the Eocene Middle Green River (MGR) Fm. in Uinta Basin, Utah, proximal-to-distal changes in the delta channel architecture are observed in previously mapped units. In the proximal MGR at Sunnyside Quarry, Utah, the units are composed of thick (10s of meters) channels which are sharp based, highly amalgamated, and with planar and trough cross-stratified beds forming large (5-10m) high-angle lateral accretion units. Following the depositional units downdip relative to the main paleo-flow direction (NW) into the Cottonwood Canyon the channels increase in number and change geometries—up to 5m thick with higher aspect-ratios (width to depth). The most distal packages of the MGR are about 40 km from proximal channels along Highway 191. These distal packages are mainly lacustrine shales with thinly bedded, occasionally channelized, laterally extensive sandstone beds. Mapping changes in geometry of singular units throughout the deltaic system (10s of kms) via drone photogrammetry and field observation will allow for the development of a predictive channel architecture framework to constrain further subsurface interpretation via well-logs and seismic imaging wherein fluvio-lacustrine channels will be largely below current interpretive resolution.
The Neales Delta distributes sediment to Australia's largest endorheic basin which has rapid base-level fluctuations (100s of years). We posit that the Neales Delta serves as a modern analogue to the large (15-25km) "Sunnyside Delta" in the Middle Green River Fm. The main distributary channel belt has a sinuous planform with a low aspect-ratio (width-to-depth) and high relief (bankfull depth of ~4m). The main distributary channel quickly radiates into tens of distributive channels that lose relief (bankfull depths of ~2m). The distal reaches of the Neales Delta (delta front) is composed of numerous interconnected unconfined channels which produce < 1m relief, forming lake delta-front sand sheets which infill shallow Lake Eyre.

Keywords: sedimentology, lakes, lacustrine, limnology, channels, green river

SHP
ECG

Mapping Variability and Distribution of Marine Isotope Substage (MIS) 5a Eolianite Deposits across San Salvador Island, the Bahamas

Scarlette Hsia
Hsia, S., The University of Texas at Austin, Austin, TX
Kerans, C., The University of Texas at Austin, Austin, TX

Understanding timing and amplitude of past sea level changes through a closer examination of late Pleistocene carbonates on San Salvador Island can inform constraints on glacio-isostasy, ice sheet distribution derivations, and earth loading deformation processes. Despite the importance of refining positioning of peak sea level highstands in the Quaternary where the most high-resolution sea-level data exists, peak global mean sea level (GMSL) remains controversial. In this study, an investigation of late Pleistocene deposits suspected to be from MIS 5a, an interglacial highstand 80 kya, is conducted through remote-sensing, petrography, and amino acid racemization (AAR). LiDAR data acquired courtesy of ExxonMobil was used as a first pass for identifying morphological differences in suspected MIS 5a deposits. Most MIS 5a eolianites are preferentially deposited along the eastern coastline and windward side of this island and eroded into headlands where Holocene strandplains have since accreted seaward and formed catenary cays. After point-counting of the 38 thin sections, averaged data from catenary cays showed dominantly skeletal bioclasts with virtually no microcrystalline calcite cement (1%) in interparticle pore spaces while MIS 5e samples were dominated by ooids and peloids with significantly more sparry calcite cement present (19%). The compositional differences do not support the idea that these eolianites were part of the regressive phase of the falling stage 5e suggested in previous studies since evidence of reworked grains such as ooids or peloids are <1% of MIS 5a. Instead, the bioclastically dominated foram-coral-skeletal-grainstones are more likely to be part of their own highstand (5a) with a different dominant sediment source and accommodation space on the isolated platform. Samples from the southeast corner of the island believed to be mantling the pisoid caliche surface that caps MIS 5a are composed of peloids and bioclastics and present great similarity to the North Point member (Holocene). Preliminary data from the Amino Acid Geochronology Laboratory in Northern Arizona suggest differentiable ranges of Glu/Asp ratios between Holocene and 5a but results for further testing on 5e samples are pending. Future work will focus on developing methods to characterize and distinguish the MIS 5a highstand as climatically differentiable from MIS 5e and sampling the paleoshoreline that outcrops under present day sea level.

Keywords: Mapping, Petrography, LiDAR, Carbonates, Sedimentology

SHP
ECG

Influence of tree water content in the zero-flow maximum temperature difference: A theoretical and experimental approach

Ana Maria Restrepo Acevedo
Matheny, A., The University of Texas at Austin, Austin, TX
Agee, E., University of Michigan, Ann Arbor, MI
Restrepo, A., The University of Texas at Austin, Austin, TX

The hydraulic performance of woody species plays an important role for productivity and survival of trees. Sap flux measurements are the most commonly used techniques for the assessment of transpiration and hydraulic response to changing environmental conditions. While multiple heat-tracer style sensor types exist, the most broadly used are Granier-style thermal dissipation sensors. There is mounting evidence that variation in wood moisture content influences the nocturnal maximum temperature (T_{max}) baseline of thermal dissipation probes. This wood moisture content variation can be assessed by multiple field measurement techniques. Traditionally, changes in stem water content have been measured by high accuracy, micron scale electronic dendrometers. New techniques leveraging on capacitance sensing technologies commonly used for collecting soil moisture data have also recently been applied at large scales to observe wood moisture content *in situ*. We pair three years of dendrometer and capacitance sensor measurements of wood moisture content with sap flux observations made using traditional thermal dissipation probes in a mixed forest in northern Lower Michigan. Our study aims to (i) evaluate the coherence between the two measures of wood moisture and to (ii) assess the influences of changes in wood water content on the T_{max} baseline at long term (seasonal) and short term (interstorm period) time scales. We also present results of a dehydration experiment which pairs measurements of moisture content from *Quercus spp* wood segments with TDP measured T_{max}. We demonstrate the species-specific influence of wood moisture content on the T_{max} baseline and suggest its applicability as a correction factor for long-term sap flux datasets.

Keywords: Sap-flux, water content, transpiration, wood moisture

SHP
ECG

Tidal formed compound clinoforms of Colorado river delta in ancient deposits of Fish Creek-Vallecito Basin and in modern Baja California

Fernando Rey
Rey, F., Jackson School of Geosciences, The University of Texas at Austin, Austin, TX

Tidally dominated environments are a key part of shallow marine, coastal and fluvial settings. This study seeks to understand and document the architecture of tidal-dominated deltas. During the early Neogene, the paleo-Colorado river was filling the Fish Creek-Vallecito Basin, now located about 200 km north of the Gulf of California. Ancestral Colorado Delta deposited Pliocene Deguynos Fm. which is exposed in Anza-Borrego State Park and provides continuous outcrops (kilometers long and hundreds of meters thick). This formation is divided (from bottom to top) into Mud Hills, Yuha and Camel Head members. Mud Hills Member (100s of m thick) is dominated by “rhythmites”, cm-thick rippled very fine sandstone alternating with mudstone (silts and clays). Preliminary work shows that Yuha Member has multiple fossil-rich sandstone units, a few meters thick each, which alternate with tens of meters thick mudstone units. Yuha sandstone beds are dominated by cross-strata at times bi-directional or with mud drapes, and dm to m thick rippled cosets. Camel Head Member, transitional to a more proximal environment, has multiple channelized sandstones, and abundant bioturbation. These two upper members are interpreted as tide-dominated (based on the facies) delta front deposits (overall thickening and coarsening uptrend). However, if we relate these deposits with the underlying Mud Hills Member, the vertical succession from hundreds of meters thick “rhythmites” to an alternation of tens of meters thick muds and meters thick sandstone locally rich in fossils point to a double clinoform (or compound clinoform) architecture. Actually, this muddy section is so thick that it is likely merging down into bathyal muddy slope deposits that host a submarine fan at their base.

The modern Colorado River Delta in Baja California, Mexico also shows a double clinoform morphology in its bathymetry. The river mouth/delta position in the northernmost end of the Gulf of California shows enhanced tidal-current velocities and the tidal range (over 10 meters) making it the dominant process in the deltaic/shallow marine environment. Satellite images and bathymetry maps reveal several classic tidal morphological features, such as tidal bars and tidal channels, and the existence of compound clinoforms associated with the progradation of the delta. In the literature, the modern deposits are strikingly similar to Pliocene Deguynos Fm., with its locally thick shell beds.

Compound clinoforms have been increasingly recognized in modern major river deltas during the last 30 years; most of them have very strong tidal process component. The compound clinoforms are composed by a subaerial clinoform (coastal plain delta) and a subaqueous clinoform (subaqueous delta) which are separated by a subaqueous platform. However, despite the ubiquity of double clinoforms in the modern tidal deltas, there are only limited examples in the ancient deposits and therefore a future objective of this research will be to link modern and ancient examples, trying to recognize the characteristics of the environments which compose the compound clinoform in the deposits.

Keywords: Tidal dominated deltas, Shallow Marine, Colorado River, Gulf of California, Compound Clinoform

SHP
ECG

Linking Geomorphology and Stratigraphy at an Ancient Fluvial Avulsion Node: An example from the Cretaceous Cedar Mountain Formation, Eastern Utah, USA

Cole Speed
Speed, C., Department of Geological Sciences, The University of Texas at Austin, Austin, TX; Bureau of Economic Geology, The University of Texas at Austin, Austin, TX
Sylvester, Z., Bureau of Economic Geology, The University of Texas at Austin, Austin, TX
Flaig, P., Bureau of Economic Geology, The University of Texas at Austin, Austin, TX
Durkin, P., Department of Geological Sciences, University of Manitoba, Winnipeg, Manitoba, Canada
Goudge, T., Department of Geological Sciences, The University of Texas at Austin, Austin, TX

Linking the modern 2D-3D geomorphologic expression of ancient channel-belt deposits to the original fluvial style is challenging, as only select portions of the channel-belt may be preserved. This is especially true in portions of fluvial systems in which stratigraphic preservation potential is expected to be low. An example of such a region is near an avulsion node, where river flow has been re-routed onto its adjacent floodplain. This process can remove evidence of the avulsion process and some pre-avulsion deposits. Although avulsions are frequent in modern fluvial systems, they are essentially instantaneous on geological timescales. Therefore, the preservation potential of deposits related to avulsion events is thought to be relatively poor. In addition, few outcrop examples exist with adequate exposures to provide the spatial and temporal context necessary to characterize the architectures and geometries of ancient fluvial avulsion node strata.

Exhumed channel-belt deposits of the Cretaceous Cedar Mountain Formation, eastern Utah, USA offer the opportunity to relate modern geomorphology to ancient stratigraphy in three-dimensions. Exhibiting relief of 5-25 m above the surrounding landscape, the coarse-grained fraction of Cedar Mountain channel-belt deposits forms a resistant barrier to erosion of underlying finer-grained floodplain facies, resulting in the formation of arcuate ridges displaying both map- and cross sectional-views of fluvial stratigraphy. We examined two intersecting ridges that we interpret as deposits of an ancient fluvial avulsion node, based on stratigraphic relationships and paleoflow indicators between ridge deposits. We analyze and interpret 3-D digital outcrop models (DOMs) produced using high-resolution photogrammetry, and map bedding geometries, sedimentary structures, and erosional surfaces on DOM-derived orthorectified photopanels. Transects of stratigraphic sections along vertical ridges are coupled with plan-view maps of outcrop exposures to document the stratigraphic architecture and vertical and lateral facies variability. Over 300 measurements of dune foresets and accretion strata are recorded from the top and along the sides of the exhumed deposits to constrain the spatio-temporal evolution of the system upstream and downstream of the hypothesized avulsion node.

Results show that the intersecting ridges document the evolution of a coarse-grained, low sinuosity meandering river breached near the apex of a relatively high curvature meander bend, subsequently depositing a northward thickening package of post-avulsion deposits onto the time-equivalent floodplain. The newly formed north-south trending channel-belt migrated laterally before final abandonment. To further tie the modern geomorphology to the preserved deposits, we implement a Python-based numerical model (MeanderPy) to reproduce the stratigraphic relationships observed in the field. Digitized channel centerlines obtained through field-based reconstruction of the interpreted channel positions are used as input to the stratigraphic forward model. Future work will examine and compare vertical slices through the 3-D volume of synthetic stratigraphy to vertical exposures observed along the Cedar Mountain ridges to further constrain the relationships between modern geomorphology and ancient stratigraphy of this avulsion. This study has significant implications for recognizing avulsion strata and for fluvial channel-belt reconstructions.

Keywords: Fluvial geomorphology, avulsion, sedimentology, stratigraphy, stratigraphic modeling

LCMS

Provenance, Geochronology and Sedimentary Characteristics of the Campanian M1 Sandstone, Oriente Basin, Ecuador

Sinong Lin
Lin, S., Jackson School of Geosciences, The University of Texas at Austin, Austin, TX
Olariu, C., Jackson School of Geosciences, The University of Texas at Austin, Austin, TX
Steel, R., Jackson School of Geosciences, The University of Texas at Austin, Austin, TX
Good, D., Andes Petroleum Company Ltd, Quito, Ecuador

The Late Cretaceous Campanian (72.1-83.6 Ma) M1 Sandstone is one of the major oil reservoirs in Oriente Basin, Ecuador. The M1 sandstone is found mainly in central and eastern parts of the basin and overall thinning direction is to the west. The relative thinness (usually under 25 meters) makes it difficult to identify the depositional patterns within the M1 sandstone through seismic data. Furthermore, M1 gamma ray logs, and even two adjacent wells with similar gamma ray pattern have different reservoir pressure values suggesting distinct reservoir units. The reservoir behavior suggests the depositional environment of the M1 sandstone is variable and contains complex compartmentalization. Hence, we combined provenance and geochronology study to complement the sedimentological observations and understand the regional deposition of the M1 sandstone. Detrital Zircon Dating has been applied to 21 core samples of the M1 sandstone across the entire basin. The probability density plot (PDP) curves of those samples provide the evidence that sediments are mainly coming from the Amazonian Craton, which are Rio Negro-Juruena Province (RNJ: 1.78-1.55 Ga) and Rondonian-San Ignacio Province (RO: 1.55-1.30 Ga). Moreover, the main M1 and upper M1 have locally distinct signatures either from RNJ or RO, such as Nantu well is missing RO peak in upper M1 while Dorine well has a shift of RNJ peak from main M1 to upper M1. The zircon analyses suggest M1 sandstone in the central and western Oriente Basin is still Craton derived, likely reworked in the basin by tidal currents. Further analysis of the age signal together with well log interpretation and core description allow a reconstruction of the sediment transport patterns. The M1 sandstone varied in its derivation direction from the Craton, initially being sourced dominantly from the south-east and later from the east. The core description and log correlation indicate that M1 sandstone was deposited in most areas under strong tidal-current influence. At beginning it developed regressively with much sediment bypass to the northwest, but was later reworked (almost completely in places) by tidal currents during transgression. The depositional model generated emphasizes the general transport direction and typical depositional elements (channels, bars, abandoned muddy tracts).

Keywords: M1 Sandstone, Oriente Basin, Detrital Zircon Dating

CCG
LCMS

Recovery After Ocean Anoxic Events: A Closer Look at the Carbonate Factory Response Preserved in The Pearsall Formation in Central Texas Following OAE 1A

Esben Pedersen
Pedersen, E., Department of Geological Sciences, The University of Texas at Austin, TX
Kerans, C., Department of Geological Sciences, The University of Texas at Austin, TX
Larson, T., Bureau of Economic Geology, The University of Texas at Austin, Austin, TX

Ocean anoxic events (OAEs) are major carbon cycle perturbations that occurred multiple times in the Mesozoic. These events are most commonly associated with the shutdown of precursor benthic carbonate factories and followed by deposition of black shales, some of which are known economic source rocks. In central Texas, OAE?related source intervals include the Pearsall and into the Glen Rose Formations (OAE?1A through OAE?1A), the Eagle Ford Formation (OAE?2), and the Austin Chalk (OAE?3). Recovery of the benthic carbonate factory following OAEs sets up the potential for encapsulated source?reservoir play systems. Post?OAE Gulf of Mexico reservoirs are known to occur in shelf interior grainstone belts (James Limestone Member of the Pearsall Formation) and in association with patch reefs (e.g., James Limestone, Bexar Shale, and lower Glen Rose Formations). While significant academic research has focused on identifying mechanisms that are responsible for the onset of OAEs, less research has focused on understanding how carbonate factories recover from these perturbations and return to an environment that fosters a healthy carbonate platform.

This study seeks to investigate the Early Cretaceous (Aptian) OAE?1A that is recorded by the Pine Island Member of the Pearsall Formation in South Texas, with a particular focus on shelf sequences preserved in both core and outcrop in a transect from the San Marcos Arch to the Pearsall Arch. When linked to detailed study of ichnofossils and macrofossils, stratigraphy, and organic carbon chemistry, this coupling of core characterization with field observations allows us to better understand the evolution and variability of carbonate facies along this transitional interface during carbonate recovery. This work aims to clarify the stratal architecture of the Pearsall Formation and to refine our understanding of the relative timing of events from the peak of biotic crisis preserved in the Pine Island Member during OAE?1A, through the partial recovery phase recorded in the deposition of the Cow Creek Formation, and to the later biotic perturbation marked by OAE?1B in the Lower Glen Rose Formation.

Considering post?OAE recovery mechanisms, the transformation from anoxic to oxygenated conditions will vary along the carbonate platform depending on depth, proximity to shoreline, and basin restriction. Unlike the onset of OAEs which appear to be sharp, recovery mechanisms from OAEs may be more gradual. Depending on shelf position and basin restrictions, carbonate deposition and fossil fauna may evolve differently. For example, slow recovery from anoxic conditions would be expected in more restricted basins, resulting in longer persistence of stressed fauna including dense oyster assemblages and burrowed mixed siliciclastic carbonate deposits. In contrast, carbonate systems in unrestricted basins may more quickly reach a condition to sustain reef structures with the potential to develop into diverse, steep?walled carbonate platforms indicative of full carbonate recovery.

Ultimately, identifying the dominant mechanisms driving recovery and transition from stressed OAE environments to sustained carbonate deposition will allow for better characterization of both conventional and resource plays by improving our predictive framework of spatial distribution of source and reservoir rocks.

Keywords: Oceanic Anoxic Events, OAE, Carbonates, Reservoir, Cretaceous, Pearsall, Gulf of Mexico

EG
LCMS

Seismic image interpolation from scattered locations to a regular grid

Ben Gremillion
Gremillion, B., Bureau of Economic Geology, The University of Texas at Austin, Austin, TX
Fomel, S., Bureau of Economic Geology, The University of Texas at Austin, Austin, TX

We propose a method to create a 3D seismic volume from traces at sparse, irregular locations. Dynamic time warping is first incorporated into a least-squares inversion scheme to find the time shifts that align reflectors at input traces. Then the aligned reflectors and their associated shifts are interpolated to a regular grid, creating a flattened seismic volume. The flattened reflectors in the seismic volume are then translated to their estimated positions using the interpolated shifts. An application of this technique to a field dataset confirms its validity.

Keywords: interpolation, seismic data processing

LCMS-4

SETP
LCMS

Characterizing the evolution of dynamic pressure resulting from the 18 May 1980 pyroclastic density current of Mount St. Helens using tree damage

Nicole Guinn
Guinn, N., Jackson School of Geoscience, The University of Texas at Austin
Gardner, J., Jackson School of Geoscience, The University of Texas at Austin
Helper, M., Jackson School of Geoscience, The University of Texas at Austin

Tree damage can provide insights into internal dynamic pressure changes of pyroclastic density currents (PDC). On 18 May 1980, Mount St. Helens erupted a laterally directed PDC that decimated ~600km^2 of forest, referred to as the blowdown zone. The head of the current contained the peak dynamic pressure, which uprooted or broke off most trees and stripped them of vegetation; however, some partially stripped tree trunks were left standing. Tree damage was assessed using aerial photography taken one month after the eruption. The flow direction of the PDC was mapped from shadows of root balls of toppled trees and directions of fallen trees. Along given flow paths, the density of standing trees was measured by the number of shadows within 200m^2 areas. The last 10% of runout illustrated a marked increase in tree density. Without the effect of topography, dynamic pressure is interpreted to decrease slowly with distance from the vent. Upon reaching a critical density threshold, the dynamic pressure drops significantly in its last 10% and the PDC lifts off into the atmosphere, leaving behind a significant number of standing trees.

Additionally, analysis identified 95 clusters of trees still standing in the blowdown zone, situated on the lee sides of hills or plateaus. Blurry, cylindrical shadows versus well-defined, cylindrical shadows distinguished standing trees with foliage in clusters from those without. The foreslope angles and hill heights were quantified to compare hills that contained patches. Stripped patches have higher foreslopes averaging at 24±10° while foliage patches averaged at 18±11°. However, hill height did not influence the patch type. Hill heights for stripped patches averaged at 64±44 m while foliage patches averaged at 63±63 m. The foreslope angles and hill heights of prominent hills that transected flow paths of hills with patches were calculated as a proxy of energy loss within the PDC. Most hills with patches had larger foreslopes and had preceding hills that are taller. Additionally, the patch type with distance from the vent revealed that topography had a major impact on dynamic pressure evolution. Hills within 50% of runout did not have patches and indicated that the peak dynamic pressure hugged topography. Stripped patches began after the first 50% of runout and implied that the peak dynamic pressure was still low enough to damage trees though the current had jumped over topography. Foliage patches began in the last 20% of runout and suggested that the peak dynamic pressure had risen above the tops of the trees. Furthermore, five variables were used to determine the heights of trees in the patches: ground slope and aspect, bearing and length of shadows, and the sun angle above the horizon. Tallest stripped trees were on average 31±18 m, and tallest foliage trees were on average 20±11 m. Tree heights in the patches indicated a localized height the peak dynamic pressure must jump as it traveled over hills and away from its source.

Keywords: dynamic pressure, pyroclastic density current, Mount St. Helens, trees, tree damage, PDC

SETP
LCMS

Constraining the tectono-thermal evolution of the Egyptian Red Sea margin: linking observations from the proximal to the hyperextended rift domain

Samuel Robbins
Robbins, S., Department of Geological Sciences, Jackson School of Geosciences, The University of Texas at Austin, Austin, TX
Stockli, D., Department of Geological Sciences, Jackson School of Geosciences, The University of Texas at Austin, Austin, TX
Bosworth, W., Apache Egypt Companies, 11, Street 281, New Maadi, Cairo, Egypt
Galster, F., Department of Geological Sciences, Jackson School of Geosciences, The University of Texas at Austin, Austin, TX

The evolution of the Red Sea rift system – one of the prototypical and conceptually most influential continental rifts - can be differentiated into several distinct rifting phases: (i) rift initiation at ~23 Ma along the entire Red Sea, (ii) onset of necking and hyperextension recorded by rapid syn-rift subsidence in the E. Miocene (~19 Ma), (iii) transition to oblique rifting and movement along the Aqaba transform in the M. Miocene (~14 Ma) likely leading to coupled hyperextension and mantle exhumation, and finally (iv) initiation of oceanic spreading in the S Red Sea at ~5 Ma. This study presents new U-Pb and (U-Th)/He data from both the proximal Egyptian margin and the distal hyperextended margin (Zabargad Island) constraining the thermal evolution during progressive continental rifting and oceanic rupture. (U-Th)/He data from transects across upper- and lower-plate portions of the Egyptian proximal margin between the Gulf of Suez and Sudan record the structural and temporal evolution of rift initiation and necking in the proximal margins. In contrast, data from the distal domain exposed on Zabargad preserves both E. Miocene hyperextension as well as Pliocene reheating during nascent oceanic spreading. Zabargad represents a rare exhumed portion of a highly-attenuated distal rifted margin that was subsequently uplifted along the oceanic Zabargad fracture zone. While zircon U-Pb data document the E. Miocene phase of hyperextension, rutile and apatite U-Pb data from basement samples, yielding ages from ~5-12 Ma, document the exhumation phase and, more significantly, the reheating of the distal margin during initial oceanic break-up. This reheating of the distal continental margin has not been documented in modern or fossil hyperextended margins. These new data provide important new constraints on the thermal and mechanical evolution of rift margins during both necking and oceanic break-up and provide critical new insights into the thermal evolution of the crust during the transition from continental hyperextension to oceanic spreading as well as the role that reheating plays in rift propagation. In summary, these new thermochronometric data from the Egyptian Red Sea provide unique new insights into the thermal evolution of progressive rifting and continental break-up of one of the most prototypical rift systems.

Keywords: tectonics, rifting, hyperextension

LCMS-6

SHP
LCMS

The chemical evolution of municipal water in the natural environment

Hunter Manlove
Manlove, H., Department of Geological Sciences, The University of Texas at Austin, Austin, TX
Beal, L., INTERA Inc., Austin, TX
Loewald, A., Middlebury College, Middlebury, VT
Mauceri, A., Macalester College, Saint Paul, MN
Banner, J., Department of Geological Sciences, The University of Texas at Austin, Austin, TX
Tremaine, D., Department of Geological Sciences, The University of Texas at Austin, Austin, TX

The city of Austin, Texas has experienced rapid population growth and urban development, posing challenges to urban watershed resilience for people who depend on surface waters to maintain water quality and quantity. Geochemical differences observed between relatively pristine rural and altered urban stream waters indicate varying degrees of containment failure within the municipal supply and waste water networks as infrastructure ages and urbanization increases. Although there is evidence for significant losses of treated water from the municipal infrastructure, little is known about the evolution of such water once it enters the natural groundwater system.

The City of Austin sources municipal water from the Lower Colorado River, which is fed by the Llano River that flows over Precambrian granite, resulting in elevated strontium isotope ratios ($^{87}Sr/^{86}Sr$ = ~0.7091) relative to Austin-area streams that incise Cretaceous carbonate bedrock ($^{87}Sr/^{86}Sr$ = ~0.7074). When leaked municipal waters infiltrate into the subsurface, the bedrock imparts dissolved constituents through water-rock interaction processes. We couple stream water cation [Ca^{2+}, Mg^{2+}, Sr^{2+}] and anion [Cl^-, Fl^-] analyses with $^{87}Sr/^{86}Sr$ at sites in seven watersheds to construct geochemical models with which to assess how increasing urbanization and population have affected Austin-area stream chemistry. As municipal waters flow into streams and creeks, strontium isotope ratios decrease through interaction with the limestone bedrock. More chemically evolved stream waters will have increased cation concentrations as water-rock interaction progresses, and waters will shift further away from the initial municipal water composition.

Waller Creek is a heavily urbanized watershed in Austin that demonstrates elevated $^{87}Sr/^{86}Sr$ closer to that of municipal water than rural streams. Waller Creek stream waters are less chemically evolved than stream waters from all seven studied watersheds and demonstrate limited water-rock interaction processes that are modeled by fluids progressively dissolving and recrystallizing calcite. The urban Waller Creek waters maintain an elevated strontium isotope ratio and low Sr/Ca compared to the more rural watersheds that either exhibit low $^{87}Sr/^{86}Sr$ and high Sr/Ca or span a range of values and degree of chemical evolution. These urbanized waters also exhibit a significant trend (R^2=0.87) of Ca to Sr that follow the modeled dissolution of the underlying Austin Chalk. The more limited geochemical evolution processes reflected in Waller Creek relative to other Austin-area watersheds may be a consequence of the low permeability and fracture-dominated flow in the chalk.

Keywords: Hydrogeochemistry, urban watersheds, isotope geochemistry

SHP
LCMS

Ice-free beaches and lagoon sediment in the Arctic coast

Micaela Pedrazas Hinojos
Pedrazas, M., Jackson School of Geosciences, The University of Texas
Cardenas, M., Jackson School of Geosciences, The University of Texas
Demir, C., Jackson School of Geosciences, The University of Texas
Watson, J., Jackson School of Geosciences, The University of Texas
Connolly, C., Marine Science Institute, The University of Texas
McClelland, J., Marine Science Institute, The University of Texas

Subsea ice-bearing permafrost assumed to underlie the many lagoons in the Arctic is prone to degradation because of rapid warming. However, subsea frozen sediment found near shore has only been sporadically directly mapped and its thawing remains undocumented. Through electrical resistivity imaging across a lagoon in northeastern Alaska, we found that the subsurface is ice-free down to at least 17 m in the lagoon and to 22 m at the beach, in contrast with other studies. This surprising result means that there is rapid melting or that ice-bearing permafrost had been absent for some time. The observations imply that the beach and lagoon subsurface are an active component of the coastal Arctic ecosystem, where there is potentially significant exchange of water, solutes and gases between the surface, the subsurface and the atmosphere.

Keywords: Permafrost, geophysics, electrical resistivity, ice, arctic aquifers

SHP
LCMS

Comparing transpiration changes of three tree species based on hydraulic strategy in a semi-arid region

Austin Rechner
Rechner, A., Jackson School of Geosciences, The University of Texas at Austin, Austin, TX
Acevedo, A., Jackson School of Geosciences, The University of Texas at Austin, Austin, TX
Romulis, C., Jackson School of Geosciences, The University of Texas at Austin, Austin, TX
Bolduc, C., Jackson School of Geosciences, The University of Texas at Austin, Austin, TX
Mursinna, A., Jackson School of Geosciences, The University of Texas at Austin, Austin, TX
McCormick, E., Jackson School of Geosciences, The University of Texas at Austin, Austin, TX
Matheny, A., Jackson School of Geosciences, The University of Texas at Austin, Austin, TX

As precipitation and temperature patterns continue to shift due to climate change, understanding if and how ecosystems and their different plant species will survive is crucial. Plants exchange water for carbon through the process of transpiration, the largest component of the terrestrial water cycle for many ecosystems. We hypothesize that species with the most advantageous combination of hydraulic traits are the most well adapted to survive. Here we use a plant hydraulics model in combination with a field study to (1) determine which hydraulic strategies are being used by different species and (2) test if these traits will better enable plants to survive droughts.

This study uses micrometeorological and sap flux data, collected using Granier-style sensors, to quantify transpiration rates in three tree species (*Pinus remota*, *Quercus laceyi*, and *Juniperus ashei*) on a semi-arid ranch located near Rocksprings, Texas, USA to compare water use rates between species under varying environmental conditions. We use these data with the finite difference ecosystem-scale tree crown hydrodynamics model version 2 (FETCH2) in order to better understand the hydraulic traits of our three study species. FETCH2 utilizes finite difference numerical methodology to determine water xylem potentials throughout a tree. Based on the assumption that xylem functions similarly to porous media, FETCH2 uses the Richards equation to account for the conductance and capacitance of the tree's hydraulic system with changes in water potential. The model can be parameterized with measured plant hydraulic traits such as xylem conductivity, isohydricity, and rooting depth to simulate the trees' different hydraulic strategies. We employ the model as a sensitivity test to analyze which suites of plant hydraulic traits are the most deterministic of the trees' observed transpiration patterns. We further expand our analysis by using the parameterized model to simulate site-wide changes in transpiration if precipitation patterns change and our study site becomes increasingly arid.

Model simulated transpiration provides insight into how our tree species obtain and utilize water. By comparing the hydraulic traits and the resulting parameter sets, we can enhance our understanding of hydraulic strategy and its influence on total transpiration as well as transpiration in response to simulated and observed droughts. As the climate continues to warm and precipitation patterns become increasingly variable, a mechanistic understanding of and ability to model species-specific vegetation responses to drought will be crucial for predicting water and carbon fluxes.

Keywords: Transpiration, hydraulic strategy, plant hydrodynamics model, sap flux

LCPHD

Integrated Airborne Geophysics Survey over a Newly-Discovered Subglacial Lake in Princess Elizabeth Land, East Antarctica

Shuai Yan
Yan, S., University of Texas Institute for Geophysics, USA; Department of Geological Sciences, Jackson School of Geosciences, University of Texas at Austin, USA
Blankenship, D., University of Texas Institute for Geophysics, USA
Greenbaum, J., University of Texas Institute for Geophysics, USA
Guo, J., Polar Research Institute of China, China
Li, L., Polar Research Institute of China, China
Young, D., University of Texas Institute for Geophysics, USA
Roberts, J., Australian Antarctic Division, Australia
Ommen, T., Australian Antarctic Division, Australia
Sun, B., Polar Research Institute of China, China

Antarctic subglacial lakes interact closely with the overlying Antarctic Ice Sheet (AIS), and could provide unique bio-geochemical environments and contain valuable sediment records. Recently, an extensive subglacial canyon and lake system has been inferred from satellite-based remote sensing in Princess Elizabeth Land (PEL), East Antarctica. This canyon system extends from the north side of the Dome Argus to the coast between Amery Ice Shelf and West Ice Shelf, two major ice shelves in East Antarctica. The subglacial lake, hereby referred as Lake Snow Eagle (LSE), is located at the upstream part of the canyon and inferred to be one of the largest lakes lying beneath the Antarctic Ice Sheet. This study, for the first time, confirms the existence of this subglacial canyon and lake system, and systematically investigates its geometry, bathymetry and geological characteristics.

The University of Texas Institute for Geophysics (UTIG), Polar Research Institute of China (PRIC), and Australian Antarctic Division (AAD) have been working closely to perform airborne geophysical surveys in Antarctica. During the collaboration, more than 10,000 kilometers' survey profiles were collected over the lake region. Data sets used in this project were mainly collected in the following expeditions: the 32nd, 33rd, 34th, and 35th Chinese National Antarctic Research Expedition (CHINARE) (2015/16, 2016/17, 2017/18, and 2018/19), and the 10th International Collaborative Exploration of the Cryosphere through Airborne Profiling program (ICECAP) (AAD/UTIG ICP10, 2018/19). The airborne survey platform houses instruments such as Ice-Penetrating Radar (IPR), gravimeter, magnetometer, and laser altimeter. Data products from these surveys provide valuable information on the ice sheet geometry, basal topography, as well as geological framework of the lake region.

Keywords: airborne geophysics survey, subglacial lake, Antarctica

CCG
LCPHD

An Integrated Framework to Model Nitrogen Leaching in a Land Surface Model: San Antonio and Guadalupe Basins

Seungwon Chung
Chung, S., Department of Geological Sciences, The University of Texas at Austin, Austin, TX
Yang, Z., Department of Geological Sciences, The University of Texas at Austin, Austin, TX
Tavakoly, A., U.S. Army Engineer Research and Development Center, Coastal and Hydraulics Laboratory, Vicksburg, MS.

Nitrogen supports global demand for food and energy production, but it may threaten water resources across the globe with eutrophication. This study presents an integrated modeling system to simulate nitrogen in soil at regional scale watersheds. It enables us to mechanistically model nitrogen that are influenced by climate and human activities as well as to quantitatively assess their impacts on the nitrogen cycle. For this purpose, the Noah-MP land surface model with terrestrial Carbon and Nitrogen dynamics (Noah-MP-CN) model and the Net Anthropogenic Nitrogen Inputs (NANI) dataset were incorporated to simulate nitrate flux leaving soil. We investigated the efficacy of this regional ecosystem modeling approach using data from San Antonio and Guadalupe Basins, which flow into the Gulf of Mexico. The San Antonio and Guadalupe Basins are ideal case study sites, because the drainage basins are covered by various types of nitrogen sources. The integrated modeling system was run over 38 years (1981-2018) at an hourly time step. The simulations are compared with various observational data sets, including the U.S. Geological Survey (USGS) streamflow and nitrate concentration data, the Moderate Resolution Imaging Spectroradiometer (MODIS)-observed leaf area index (LAI) data, the Soil Moisture Active Passive (SMAP)-observed soil moisture data, the FLUXCOM evapotranspiration (ET) and net ecosystem exchange (NEE) data.
The nitrogen dynamics model performs well in capturing the major nitrogen state/flux variables, including nitrate leaching. This model shows the improvement of carbon cycle modeling performance by reducing bias (e.g. leaf area index, net ecosystem exchange).

Keywords: land surface model, nitrogen cycle, nitrogen leaching, Noah-MP, Noah-MP-CN

CCG
LCPHD

Characterizing buoyant conditions of marine-terminating glaciers in West Greenland

Sophie Goliber
Goliber, S., Institute for Geophysics, The University of Texas at Austin, Austin, TX
Catania, C., Institute for Geophysics, The University of Texas at Austin, Austin, TX

There is significant heterogeneity in the amount and duration of terminus retreat and style for Greenland marine-terminating glaciers making them difficult to represent in ice sheet and glacier models. As these glaciers sit at the ice-ocean boundary, they exhibit a complex response to the myriad processes acting upon them. Two major styles of calving have been identified for West Greenland glaciers through remote sensing of terminus change; full-thickness buoyant fracture and serac failure. The former is expected to happen at glaciers that are close to or at floatation. For these glaciers, basal crevasses form at the grounding line and propagate upward where they connect with surface crevasses as they are advected to the front of the glacier, promoting calving of large tabular icebergs. The latter style of calving results from undercutting of the glacier terminus, possibly through melt, which causes surface crevasses to weaken the ice resulting in serac failure. Here we present a time series of the spatial pattern of buoyancy conditions for several glaciers in central west Greenland using Polar Geospatial Center's ArcticDEM strips from 2012-2017 in order to highlight the differences in buoyant conditions between these two different calving types. Preliminary results confirm floating conditions for those glaciers that experience full-thickness calving events. Further, we use the height above buoyancy to determine the penetration height of basal crevasses in order to understand how these vary across different glaciers.

Keywords: glacier, Greenland, glacier calving, remote sensing

CCG
LCPHD

ZooMS in the New World: The Need for a North American Faunal Database

Erin Keenan Early
Keenan Early, E., Jackson School of Geosciences, The University of Austin, Austin, TX
Shanahan, T., Jackson School of Geosciences, The University of Austin, Austin, TX
Collins, M., Natural History Museum of Denmark, University of Copenhagen

My project seeks to improve taxonomic identification of North American Pleistocene and Holocene fauna from paleontological and archaeological assemblages. High fragmentation often results in the greater portion of a faunal assemblage being taxonomically unidentifiable. ZooMS could address this problem, but the lack of a ZooMS database for North American taxa means this valuable identification tool is not meaningfully available for North American assemblages. The potential value of such a database is demonstrated by analysis of a zooarchaeological assemblage from the Gault Site in Bell County, Texas. Using MALDI-TOF mass spectrometry, I generated peptide mass fingerprint data for multiple unidentified bone fragments from this site and analyzed them using the existing ZooMS database. While some restricted identifications where possible, the majority of the fragments remain unidentified. This is exemplified by a fragment that appears to be canid when compared to the existing database. However, the spectrum does not fully match the database canid species of dog, gray wolf, red fox, or arctic fox, nor does it match non-database preliminary peptide mass fingerprint data I have taken for coyote. The inability to match this bone fragment to a canid species using the database and preliminary fingerprint data indicates that the fragment originates from an animal that gives a canid signal but has not yet been analyzed, and so is not currently identifiable. Overall, this and other Gault Site faunal fragments serve as excellent examples of both the information to be gained by the application of ZooMS and the intense need for a database of North American taxa.

Keywords: paleontology, proteomics, mass spectrometry, Pleistocene, Holocene

CCG
LCPHD

Development of plant hydraulics in the Noah-MP land surface model

Lingcheng Li
Li, L., The University of Texas at Austin
Yang, Z., The University of Texas at Austin
Matheny, A., The University of Texas at Austin
Zheng, H., Chinese Academy of Sciences
Swenson, S., National Center for Atmospheric Research
Lawrence, D., National Center for Atmospheric Research
Barlage, M., National Center for Atmospheric Research
Yan, B., The University of Texas at Austin

Plants with different hydraulic traits have different water use strategies. Isohydric plants such as maple trees exert tight stomata regulation to minimize transpiration. In contrast, anisohydric plants such as oak trees tend to tolerate low leaf water content and keep transpiration longer. These diverse plant hydraulics behaviors could have different effects on the carbon-water cycle and land-atmosphere interaction. However, plant hydrodynamics is currently excluded from most large-scale land surface/global earth system models. In this project, we develop a plant hydrodynamics module (an electric circuit analogy module, i.e., EC module) for the Noah-MP land surface model, a primary model employed in the NASA Land Information System, the next phase North American Land Data Assimilation System, and also the National Water Model. This newly developed model is evaluated using the observations (e.g., sap-flux, stem water storage, latent heat, soil moisture) from the University of Michigan Biological Station (UMBS). The evaluation is conducted at different scales (i.e., the stand level, species level, and tree level). This updated Noah-MP model with plant hydrodynamics showed better performance than the default Noah-MP model. The augmented Noah-MP model can help better understand the role of plant hydrodynamics on the global climate system and water-carbon cycles, and also makes it possible to assimilate vegetation-centric remote sensing products for data assimilation systems.

Keywords: Plant Hydraulics, Large-scale modeling, Carbon-Water cycles

CCG
LCPHD

Northern Hemisphere climate controls the northernmost limit of the Southern Hemisphere westerlies on orbital to millennial timescales

Natallia Piatrunia
Piatrunia, N., University of Texas at Austin, Austin, TX
Shanahan, T., University of Texas at Austin, Austin, TX
Augustinus, P., University of Auckland, Auckland, NZ

The Southern Hemisphere westerly wind belt (SHWW) is a key component of the Earth's climate system, responsible for the heat and energy transport through the mid and high latitudes of the Southern Hemisphere (SH) and for ocean-atmosphere CO_2 exchanges in the Southern Ocean. However, the long-term behavior of this system is poorly understood because of conflicting proxy reconstructions of the past SHWW behavior and inconsistent results from climate modeling experiments. Here, we reconstruct changes in the mid-latitude hydroclimate in the southern Pacific sector using compound-specific hydrogen isotope (δD_{wax}) and branched GDGT-derived temperature from Lake Pupuke, New Zealand (36°78.30'S, 174°76.70'E) spanning the last 45 kyr. Based on our investigation of δD data in modern precipitation, we interpret our δD_{wax} as reflecting changes in the moisture source contributions associated with variations in the northern limit of the SHWW. We find that temperature variations at Lake Pupuke are synchronous and coherent with Antarctic temperature on orbital and millennial timescales – suggesting coherent, hemispheric-wide temperature variability over at least the last 45 kyr. However, changes in the SHWW derived from δD_{wax} variations show a response that is more consistent with Northern Hemisphere climate changes; including southward shifts in the SHWW position during Heinrich stadials and an abrupt northward expansion during the Bølling-Allerød. The decoupling between the SH climate and the position of the SHWW suggests that the Northern Hemisphere climate exerts a dominant control over the SHWW, irrespective of changes in the SH mid to high-latitude climate conditions. We propose that these changes are driven by the Hadley circulation adjustment in response to the perturbations in the northward, cross-equatorial heat transport of the Atlantic Ocean, altering the strength of the SH subtropical jet leading to changes in the position of the SHWW.

Keywords: Hydrogen isotopes, brGDGT biomarkers, SH westerlies, NZ climate

CCG
LCPHD

Evolution of Mesoscale Convective Systems in the Southern Great Plains in the Last 20,000 Years: the Role of the Low-Level Jet

Chijun Sun
Sun, C., Department of Geological Sciences, The University of Texas at Austin, Austin, TX
Shanahan, T., Department of Geological Sciences, The University of Texas at Austin, Austin, TX
DiNezio, P., Institute for Geophysics, The University of Texas at Austin, Austin, TX

The extreme droughts and floods of the last decade on the North American southern Great Plains have had substantial socio-economic, environmental and ecological impacts. However, it remains unclear how the climate of this region will evolve in response to future anthropogenic forcing. Sedimentary records preserving the isotopic signals of past precipitation can inform us of past changes in hydroclimate, enhancing our understanding of the hydroclimate system of this region. Here we generated a 20,000-year record of ????D_{wax} using sediments from Hall's Cave in Central Texas. We interpret changes in ????D_{wax} as an indicator of changing convective storm activity in association with changes in the intensity of the Great Plains Low-Level Jet (LLJ). Our reconstruction shows an abrupt intensification of large scale convection during the deglaciation, followed by an early-mid Holocene drying, and a gradual return to wet conditions in the late Holocene. This temporal pattern is in agreement with changes in LLJ intensity, as simulated in the Transient Climate of the Last 21,000 (TraCE-21ka) experiments. We hypothesize that the deglacial intensification of the LLJ is associated with the saddle collapse of the North American Ice Sheets, whereas the early-mid Holocene drying is driven by the impact of orbitally forced changes in springtime insolation on land surface heating and the seasonal development of the LLJ. The TraCE-21ka experiments suggest that these changes in boundary conditions affect the geostrophic LLJ wind intensity by modifying the zonal pressure gradient between the Southern Rockies and North Atlantic Subtropical High. Although greenhouse gases appear to have played a smaller role relative to the ice sheets and insolation in controlling the hydroclimatic variability over the past 20kyr, instrumental data suggests a similar connection between an intensified LLJ/convective storms and a steeper zonal pressure gradient in response to anthropogenic warming. The Hall's Cave record highlights the sensitivity of the LLJ-southern Great Plains hydroclimate system to surface warming and zonal pressure gradients on centennial to millennial timescales.

Keywords: hydrogen isotope, paleoclimate, southern Great Plains

CCG
LCPHD

What can we expect from multi-sensor data assimilation for hydrological simulation?

Wen-Ying Wu
Wu, W., ackson School of Geosciences, The University of Texas at Austin, TX, USA
Yang, Z., ackson School of Geosciences, The University of Texas at Austin, TX, USA
Zhao, L., ackson School of Geosciences, The University of Texas at Austin, TX, USA
Lin, P., ackson School of Geosciences, The University of Texas at Austin, TX, USA

Streamflow is critical components of the water cycle and, reflecting integrated information on dominant hydrologic processes over the entire watersheds. Gauges precisely measure streamflow, but the large-scale spatiotemporal variation in streamflow is poorly understood. We evaluate the impact of multi-sensor land data assimilation on intraseasonal-to-interannual availability of runoff. Eight experiments with the assimilation of different combinations of satellites datasets are conducted using Community Land Model version 4 (CLM4) and Data Assimilation Research Testbed (DART). Different land states are updated upon the assimilated satellites observations (AMSR-E, MODIS, and GRACE) for 2003-2009. We evaluated monthly results with new GRACE dataset (CSR Global Mascons), and streamflow measured by gages using linear cross-correlations for skills. Assimilation of MODIS snow cover fraction affects simulated runoff in mid- and high-latitudes. Assimilation of lower frequencies AMSR-E brightness temperature plays an important role in soil moisture and therefore runoff in tropics. Generally, assimilating different satellite observations shows a spatially different impact on runoff, and the combination of multiple satellite observations shows the largest spatial extent. We also quantify the impact of data assimilation by evaluating results with observation-based runoff and streamflow from GRDC. Our results suggest that land data assimilation of any of these datasets improve runoff estimation over the Arctic. This study indicates the limitation of modeling the large-scale hydrological cycle and shows how data assimilation can help improve streamflow estimation.

Keywords: Global Climate Model, Remote Sensing

EG
LCPHD

Convolutional Neural Networks for Semantic Segmentation of Micro-Pores in SEM Based Images of Shales

Ken Ikeda
Ikeda, K., Jackson School of Geosciences, The University of Texas at Austin, Austin, TX
Ko, L., Bureau of Economic Geology, The University of Texas at Austin, Austin, TX
Goldfarb, E., Jackson School of Geosciences, The University of Texas at Austin, Austin, TX
Tisato, N., Jackson School of Geosciences, The University of Texas at Austin, Austin, TX

Geoscientists have increasingly been exploring unconventional shale plays. Shales have complex micro-porosity controlling their permeability and mechanical properties. Because of this complexity, the quantitative study of shale pore-space is challenging. One way to study pore spaces is by using ultra-high-resolution images that are collected using Scanning Electron Microscopy (SEM). Unfortunately, the quality of SEM images can be poor and noisy. For this reason, pore spaces in SEM images cannot simply be identified by a threshold-based method (i.e., segmentation). Semi-automatic segmentation algorithms such as a top-hat filter are ineffective because of noise. So far, labeling shale pore spaces requires effort from tracing each void space by hand. Recently, convolutional neural networks (CNNs) have demonstrated success in image recognition. Deep stacks of convolutional filters and nonlinear transfer functions allow the networks to identify complex features. Here, we show the results of a trained CNN for detecting pore spaces in shale SEM images. Sixty-nine SEM images were taken by combining the secondary electrons and the backscattered electron signals in order to reduce the charging effect. The resolution of the images ranges from 0.0024 microns-per-pixel to 0.0575 microns-per-pixel. Forty-two images of size 884 x 1024 pixels were used to train the network. Pore spaces are then manually segmented by hand. Normalization, subsampling, and image augmentation are applied to the dataset in order to avoid overfitting during the training process. We compared six CNN architectures in segmenting SEM images. The best architecture, the modified Unet with ResNet34, yields 91% accuracy of the testing dataset. In addition, the network takes less than three minutes to segment an image on a personal laptop. The trained network gives a fairly good accuracy on another set of SEM data collected from the Nankai Trough, Japan. Still, the algorithm performance on SEM images from other geological settings has to be improved and further investigated. This technique leads to a more consistent method to segment shale samples quantitatively.

Keywords: Machine Learning, Shale, SEM, segmentation

EG
LCPHD

Seismic data interpolation using deep learning

Harpreet Kaur
Kaur, H., Bureau of Economic Geology, The University of Texas at Austin, Austin, TX
Pham, N., Bureau of Economic Geology, The University of Texas at Austin, Austin, TX
Fomel, S., Bureau of Economic Geology, The University of Texas at Austin, Austin, TX

We propose an algorithm for seismic data interpolation using generative adversarial networks (GANs), which are a type of deep neural networks. The method works by extracting feature vectors of the training data by self-learning and does not require any pre-processing to create the training labels. The algorithm does not make any assumptions about linearity of events or sparsity of the data that are often included in the traditional interpolation methods. We create the training labels by randomly removing traces from different receiver indices of the original data sets to simulate the effect of missing traces. We adopt the framework of CycleGAN algorithm to train the network and add additional loss functions to regularize the model. Numerical examples using land and marine field-data sets demonstrate the validity and effectiveness of the proposed approach. With a small computational burden, the proposed method can achieve accurate interpolation results and can easily be applied to 3D seismic data sets.

Keywords: deep learning, GANs, interpolation

EG
LCPHD

Exploring Variations of Deep-Water Channel Trajectories and their Impact Upon Stratigraphic Architecture Using Channel Kinematics

Paul Morris
Morris, P., DGS
Sylvester, Z., BEG
Covault, J., BEG
Mohrig, D., DGS

Deep-water channel belts form the fundamental sand-rich building blocks of continental margins and can host valuable minerals and resources. We explore a range of stratigraphic architecture styles that can be observed on continental margins and then show how a forward stratigraphic model based on recreating kinematic processes of a geomorphic channel is able to simulate their evolution - demonstrating the overall 3D path a geomorphic channel takes as a key control upon the resultant stratigraphic architecture created. Using seismic reflection data to support the forward stratigraphic model, we quantify how apparent local variations in the overall trajectory within a channel-belt can be similar to differences observed in comparing entirely different channel-belt systems. We go on to show that the magnitude of local variations in a trajectory within a channel-belt is controlled by i) the sinuosity threshold the geomorphic channel reaches before cut-off processes begin to occur and ii) the maturity of the belt. We show how variability in sand-body stacking through the typical evolution of a channel-belt initially increases rapidly, driven by meander expansion processes of the geomorphic channel, this within-belt variability gradually reducing as the channel-belt matures by a combination of channel cut-off and translational processes. This work has implications upon furthering the understanding of processes underlying the evolution and resulting stratigraphic architecture of deep-water channel-belt systems along continental margins in addition to their associated sand-body stacking patterns.

Keywords: Channel-Belts, Forward Stratigraphic Modeling, Turbidites, Deep-water, Stratigraphy, Geomorphology,

LCPHD-12

EG
LCPHD

ANISOTROPY CORRECTION OF RECORDED SONIC LOGS

Son Phan
Phan, S., Institute for Geophysics, The University of Texas at Austin, Austin, Texas
Sen, M., Institute for Geophysics, The University of Texas at Austin, Austin, Texas

Sonic logs measured along different deviational wellbores into similar intervals of shaly sandstone might differ due to fluid content and the induced anisotropy effect, which results in scattering property distributions in well log analyses. This study introduces a calibration method to eliminate such phenomenon to the recorded acoustic signals. A set of three wells with observed significant variation in recorded P-wave velocity from similar reservoir intervals is used for demonstration purpose. The process involves first converting from measured P-wave velocity into the symmetry axis values using the Thomsen weak vertical transverse isotropic equation, then performing fluid substitution modeling to remove the fluid effects on velocity readings. The resulting log values after calibration converges toward an expected distribution. This suggests a necessary workflow to perform data QC before performing any further reservoir characterization analyses, such as estimating shear wave velocities, seismic well tie or any more advanced quantitative interpretations.

Keywords: Anisotropy correction, sonic log, data conditioning

LCPHD-13

EG
LCPHD

Correlation analysis of fracture arrangement in space: Quantified fracture (joint) clustering in Archean basement, Teton Canyon, Wyoming

Qiqi Wang
Wang, Q., Jackson School of Geosciences
Laubach, S., Bureau of Economic Geology
Gale, J., Bureau of Economic Geology
Ramos, M., Chevron ETC

We demonstrate statistically significant self-organized clustering over a length scale range from 10^{-2} to 10^{-1} m for north-striking opening-mode fractures (joints) in Late Archean Mount Owen Quartz Monzonite. Spatial arrangement is a critical fracture network attribute that until recently has only been qualitatively assessed. We use normalized fracture intensity plots and the Normalized Correlation Count (NCC) method of Marrett et al., 2018 to quantitatively discriminate clustered from randomly placed or evenly spaced patterns over a wide range of length scales and to test the statistical significance of the resulting patterns. We propose a protocol for interpreting NCC diagrams generated by the freely available NCC software CorrCount. Results illustrate the efficacy of NCC to measure clustering patterns in joints in texturally homogeneous Archean granitic rock in a setting distant (>2 km) from folds or faults. Our spectacular example of clustering is in a readily accessible exposure. These regional joints are conduits for water flow in their current geologic setting, and their patterns may be useful guides to spatial arrangement style and clustering magnitude in other, less accessible fractured basement rocks.

Keywords: Naturally fractured reservoirs, Fracture analysis, basement reservoir, statistical analysis

MG
LCPHD

Prograding clinoforms in outcrop, Mid-Jurassic Neuque?n Basin, Argentina

Yuqian Gan
Gan, Y., Jackson School of Geosciences, The University of Texas at Austin, Austin, TX
Steel, R., Jackson School of Geosciences, The University of Texas at Austin, Austin, TX
Olariu, C., Jackson School of Geosciences, The University of Texas at Austin, Austin, TX
De Almeida Jr., F., Geology Department, Universidade do Vale do Rio dos Sinos, Brazil

While seismic data give invaluable architectural information on deep water slope channels, detailed facies of slope channel fill and its relation to the architecture and the source to sink system is best studied in outcrop. La Jardinera area in south Argentinian Neuquén Basin exposes complete shelf-slope-basin-floor deposits of a prograding-dominant basin-margin clinoform system of 300 m height, formed during the early Jurassic back-arc stage. Field and remote sensing methods reveal the slope channel fill and architecture variations throughout the slope system and its linkage to to shelfal and basin floor deposits. Most slope channels exposed are single channel elements with a thickness of tens of meters, and are filled with a variety of sediment density flow deposits, including poorly sorted conglomeratic debrite, structureless high-density sandy turbidite, and sorted, fine grained, graded low-density turbidite. A grain-size analysis reveals an irregular downslope fining trend of turbidite/debrite beds in slope channel fill, except some notable bypass of conglomeratic facies to the lower most slope channels and basin-floor fans. The infill architecture of slope channels shows an apparent increase in degrees of vertical aggradation downslope. The La Jardinera system serve as a novel case study for sediment delivery in water-depth limited (<500m), prograding dominant basins.

Keywords: Clinoform, facies, sediment gravity flow, shelf processes

MG
LCPHD

Evolution and Structure of Upper Oceanic Crust in the western South Atlantic from Seismic Velocities, Gravity Data, and Hydrothermal Modeling

Dominik Kardell
Kardell, D., UTIG, Jackson School of Geosciences
Christeson, G., UTIG, Jackson School of Geosciences
Estep, J., Texas A&M University, Department of Geology & Geophysics
Zhao, Z., UTIG, Jackson School of Geosciences
Reece, R., Texas A&M University, Department of Geology & Geophysics
Hesse, M., DGS, Jackson School of Geosciences
Carlson, R., Texas A&M University, Department of Geology & Geophysics

Compared to continental crust, we think of oceanic crust as having a fairly simple, layered structure. Furthermore, it is commonly depicted as remaining relatively dormant between its formation at spreading centers and destruction at subduction zones. Hence, most studies examining oceanic crust largely focus on plate margins rather than their interiors. Here we present perspectives from multiple geophysical modeling projects that paint a much more dynamic picture of oceanic crust. Our work investigates a ~1,500 km-long transect covering slow to intermediate spreading rate oceanic crust in the western South Atlantic, aged from 0 to 70 Ma. Extensive tomographic velocity modeling using a large seismic dataset revealed a steady increase in upper crustal seismic velocities with age, providing evidence for ongoing hydrothermal activity affecting the physical properties of old crust. From a structural perspective, seismic images, full-waveform modeling, and high-resolution bathymetry depict several recently active extensional faults that penetrate well into old crust. We aim to complement our results by building hydrothermal models that may reveal the longevity and detailed geometry of fluid flow at selected localities along the transect. Aside from providing new insights into the evolution and structure of mature ocean crust, our results will also serve as a geophysical framework for an upcoming drilling expedition, which will sample upper oceanic crust along the transect at five different ages.

Keywords: Oceanic crust, marine geophysics, hydrothermal systems

LCPHD-16

MG
LCPHD

Episodic Fluid Expulsion From Gas- and Hydrate-Bearing Sands in the Terrebonne Basin,WR-313, Northern Gulf of Mexico

Patrick Meazell
Meazell, K., Department of Geological Sciences and the Institute for Geophysics, The University of Texas at Austin
Flemings, P., Department of Geological Sciences and the Institute for Geophysics, The University of Texas at Austin

Gas mounds in the Terrebonne Basin in the Walker Ridge protraction area (Blocks 313 & 269) overlie gas wipeout zones that link to the underlying Blue, Orange, and Green gas- and hydrate-bearing sand bodies. We interpret the seismic stratigraphy of the Terrebonne Basin to elucidate the origin, timing, and consequences of the processes that led to formation of these 1 km diameter fluid expulsion features. A regional bottom-simulating reflector (BSR) is elevated in the vicinity of the gas mounds. Directly beneath the mounds, a gas wipe-out zone extends downward to the dipping sand bodies and terminates at the base of hydrate stability. Below the hydrate stability zone, strong negative-amplitudes within the dipping sands record a gas column up to 450m high. We interpret that the base of the hydrate stability zone within the sand body acts as a transient seal to gas flow: it contains gas to a critical column height and then leaks gas vertically forming the gas wipe-out zone. We interpret that the base of the hydrate stability zone and hence the leak point migrated through time. Initial expulsion originated within the Blue Sand, at a point directly above the position of the regional BSR. When pressures reach a critical point, the seal is breached and warm fluid and sediments migrate vertically to the surface. The expulsion process raises the local base of hydrate stability, and a new hydrate seal forms at shallower depths. This process has repeated four times, with each resulting fluid expulsion feature progressively migrating to areas of less overburden. The timing of mound formation is such that the oldest mounds are overlying areas of greater overburden, while the more recently formed mounds have a shorter path from the gas reservoir to the surface due to the locally raised base of hydrate stability.

Keywords: Fluid expulsion, gas hydrates, Gulf of Mexico, stratigraphy

PS
LCPHD

A Novel Way to Estimate Wave Speeds of Extraterrestrial Rocks

Eric Goldfarb
Goldfarb, E., Jackson School of Geosciences, The University of Texas at Austin, Austin, TX
Eckley, S., Jackson School of Geosciences, The University of Texas at Austin, Austin, TX
Ikeda, K., Jackson School of Geosciences, The University of Texas at Austin, Austin, TX
Ketcham, R., Jackson School of Geosciences, The University of Texas at Austin, Austin, TX
Alamoudi, O., Jackson School of Geosciences, The University of Texas at Austin, Austin, TX
Tisato, N., Jackson School of Geosciences, The University of Texas at Austin, Austin, TX

Measuring physical properties of terrestrial rocks is a straightforward process: samples are collected, prepared, and measured in a laboratory setting. Measuring physical and elastic properties such as porosity, density, mineralogy, bulk modulus, shear modulus, or wave speed requires samples to be of a specific shape, and therefore the tests are physically invasive and destructive to the sample. Rock physics testing and modeling is useful. It is the primary technique by which recorded data from a large-scale geophysical survey can be tied to real samples.

With Martian seismic data from the InSight lander returning to Earth, understanding wave speeds on the red planet is a crucial step towards characterizing the structure of the Martian subsurface—one of the major objectives of the InSight mission. While samples of Martian crustal material exist on Earth in the form of meteorites, these samples are rare, small, and have irregular shapes. It is difficult to measure rock physics properties on samples of this nature – especially because we do not want to alter them.

X-ray micro computed tomography (CT) scanning allows for the collection of detailed 3D models of X-ray attenuation. These 3D models are often used to represent the physical makeup of a sample. We propose a method of converting CT models to density, porosity, and elastic properties. By scanning samples alongside phantoms of known density, a calibration curve can be made to convert X-ray attenuation to density. Porosity is estimated from its inverse relationship to density. Elastic properties can be estimated using effective medium theory. Lastly, wave speed can be estimated using the finite difference method, where wave propagations can be simulated through the 3D model. These models can all be numerically cropped, which spares the rare samples invasive laboratory preparation.

We have created and calibrated our digital rock physics model with variably shocked-metamorphosed basalt from Lonar Crater on the Deccan Traps—an analogue for the Martian surface. Numerical estimations match laboratory measurements for the physically prepared Lonar Crater samples. We then use the same numerical method to estimate properties for samples from the Martian surface. This type of noninvasive testing is possible for other rare samples, including meteorites of other origins.

Keywords: Mars, Computed Tomography, Rock Physics, Seismic, Digital Rock Physics

PS
LCPHD

Ries Central Basin as Resolved by High Resolution Seismic Profiles

Naoma McCall
McCall, N., University of Texas Institute for Geophysics, Jackson School of Geosciences, The University of Texas at Austin, Austin TX
Gulick, S., University of Texas Institute for Geophysics, Jackson School of Geosciences, The University of Texas at Austin, Austin TX
Sarv, K., University of Tartu, Department of Geology, Tartu, Estonia
Jõeleht, A., University of Tartu, Department of Geology, Tartu, Estonia
Wilk, J., University of Freiburg, Institute of Earth and Environmental Sciences, Freiburg, Germany
Pösges, G., Geopark Ries, Harburg, Germany

The 15 Ma, 26 km wide Ries Crater in Southern Germany is a well preserved, mid-sized complex impact crater. Impact craters are traditionally categorized as simple or complex. Simple craters are small, deep, and bowl-shaped, while complex craters are larger, shallow, and have either a central peak, a peak ring, or a peak ring and additional ring-shaped features. Ries is near the 25-30km threshold to form a peak ring, however current interpretations identify a crystalline ring formed by an upturned crater rim but not a true peak ring formed by material outwardly collapsing from a central uplift. Up to 300m of melt bearing impact breccia, called suevite, covers the central basin of the crater. Proposed suevite deposition processes include fallback from an impact plume, melt flow, impactoclastic density current, and melt-coolant interaction. The crater has been filled in by lacustrine sediments which have preserved the crater from erosion but the subsurface structure of the crater is poorly known. Data are limited to 1970s and earlier drill cores and logs and a low-frequency, crustal-scale reflection line. Despite being one of the most geologically studied impact craters on Earth, it had not been previously imaged with high-resolution seismic reflection.

In August 2017, we collected 4 seismic profiles at Ries Crater, Germany, imaging one half of the crater profile from outside the southern crater rim to the crater center. The seismic source was an Earth tamper capable of visualizing reflections 1.5 km deep. The tamper generated about 300-500 compressions over a 45 second listening period. Our acquisition configuration had 72 channels with 5 geophones each and channel spacing at 10 m. Maximum offset from source to receiver was 710 m.

We present the first seismic profiles from Ries crater in many decades. These high-resolution data image post impact sediments, suevite and basement showing the subsurface morphology. Geometry of the reflectors in the suevite within the crater is suggestive of deposition as lateral flows, which points to a ground hugging density currents (impactoclastic flows) rather than deposition from fallout. Topographic highs expressed in the basement are interpreted as expressions of the crystalline ring, which is not a peak ring, and a collapsed central uplift. This morphology places Ries Crater near the upper limit of a central peak crater.

Keywords: Impact Cratering, Seismic Reflection, Planetary Surface Processes,

LCPHD-19

SETP
LCPHD

Dating ductile deformation in the Maria fold-and-thrust belt with apatite and zircon U-Pb geochronometry, Big Maria and Riverside Mountains, southeastern California

Megan Flansburg
Flansburg, M., Dept. of Geological Sciences, The University of Texas at Austin, Austin, TX
Stockli, D., Dept. of Geological Sciences, The University of Texas at Austin, Austin, TX
Singleton, J., Dept. of Geology, Colorado State University, Fort Collins, CO

The Maria fold-and-thrust belt (MFTB) in southeastern California is a unique S- to SW-verging remnant of the Sevier to Laramide-age fold-and-thrust system of the North American Cordillera. The Big Maria Mountains preserve Cretaceous to Paleocene contractional and extensional deformation of the MFTB that was not overprinted by subsequent Miocene extension within the Colorado River Extensional Corridor (CREC). Ductile deformation preserved in the Big Maria Mountains provides the opportunity to robustly constrain the timing of Late Cretaceous-Paleocene deformation. To constrain ductile deformation, the preliminary work presented here provides zircon U-Pb crystallization ages of variably deformed, pre-kinematic Jurassic (~170-155 Ma) granite plutons and of syn- to post-kinematic undeformed Cretaceous-Paleocene (~85 – 64 Ma) diabase plutonics rocks and andesite and granitic pegmatite dikes which cross-cut both the Jurassic plutons and the highly attenuated and metamorphosed Paleozoic Grand Canyon sedimentary section exposed in the overturned Big Maria syncline. Further, apatite U-Pb ages of top-NE greenschist facies mylonitic shear bands within the Jurassic granitic plutons of the Big Maria Mountains are ~75-64 Ma, suggesting that the middle crust exposed in the MFTB cooled below ~450°C in the latest Cretaceous to earliest Paleocene. To the north, the Riverside Mountains preserve MFTB fabrics within the footwall of the Miocene Whipple-Riverside detachment fault system, providing the opportunity to examine and date mylonitic fabrics with in-situ titanite and apatite U-Pb petrochronology that record Late Cretaceous-Paleocene deformation as well as Miocene deformation associated with metamorphic core complex formation. Constraining deformation associated with the end of orogenesis in the North American Cordillera is critical to understanding the thermal history of the mid-crust and the role of tectonic inheritance in subsequent Miocene detachment faulting and metamorphic core complex formation in the CREC and the southern Basin and Range.

Keywords: metamorphic core complex, Cordillera, mylonite, U-Pb geochronology

LCPHD-20

SETP
LCPHD

Provenance of the Newark and Gettysburg Basins during Progressive Rifting and Continental Breakup along the Eastern North American Margin, U.S.A.

Zachary Foster-Baril
Foster-Baril, Z., Jackson School of Geosciences, The University of Texas at Austin, Austin, TX
Stockli, D., Jackson School of Geosciences, The University of Texas at Austin, Austin, TX
Bailey, C., Jackson School of Geosciences, The University of Texas at Austin, Austin, TX

Mesozoic rift basins of the Eastern North American Margin (ENAM) span from Florida to the Grand Banks of Canada and formed during progressive extension prior to continental breakup and the opening of the north-central Atlantic. While the proximal rift basins are exposed in the western portions of the ENAM, the more distal basins are deeply buried by post-rift passive margin sequences to the east. The proximal syn-rift strata from all the individual basins, lumped along the entire margin into the Newark Supergroup, are dominated by fluvial conglomerate and sandstone, lacustrine siltstone, mudstone, and abundant alluvial conglomerate and sandstone lithofacies. Deposition of these syn-rift sedimentary rocks was accommodated in a series of half grabens and subsidiary full grabens situated within the Permo-Carboniferous Appalachian orogen. The Mesozoic ENAM is commonly depicted as a magma-rich continental rift margin, with magmatism (CAMP) driving continental break-up. While the southern portion of the ENAM shows evidence of magmatic break up (e.g., seaward dipping reflectors), rifting and crustal thinning appears to start ~30 Myrs prior to CAMP emplacement in the Jurassic. This study provides extensive regional detrital zircon U-Pb provenance data, detailed stratigraphy, and bedrock zircon (U-Th)/He data to elucidate the strain evolution, the timing of crustal necking and abandonment of proximal rift basins, the provenance evolution and its implication for overall rift configuration and asymmetry during progressive rifting along the ENAM.

New detrital zircon U-Pb results from sandstone outcrop and core samples from the Newark and Gettysburg Basins indicate a distinct provenance shift with Carnian syn-rift strata predominately sourced from the east, while Norian and Rhaetian strata were regionally sourced from the western rift margin. In contrast, Jurassic strata deposited during and after CAMP magmatism in the Newark Basin are sourced from local footwall terranes. These results in conjunction with prior results from the Culpeper Basin suggest two major provenance changes during progressive rifting – the first occurring during Carnian crustal necking and a second change occurred at the onset of the Jurassic due to regional and local thermal uplift during CAMP magmatism.

Keywords: detrital zircon, provenance, progressive rifting, ENAM, Triassic, Jurassic

LCPHD-21

SETP
LCPHD

Sediment source exhumation and dispersal to the Late Cretaceous-Paleogene Mexican broken foreland from detrital zircon U-Pb-He double dating

Cullen Kortyna
Kortyna, C., Department of Geological Sciences, The University of Texas at Austin, Austin, TX
Stockli, D., Department of Geological Sciences, The University of Texas at Austin, Austin, TX
Covault, J., Bureau of Economic Geology, The University of Texas at Austin, Austin, TX
Lawton, T., Bureau of Economic Geology, The University of Texas at Austin, Austin, TX

Late Cretaceous-Paleogene inversion of the Jurassic-Early Cretaceous Chihuahua and Sabinas extensional basins in NE Mexico segmented the Mexican foreland into two sediment-routing systems: the Parras-La Popa routing system between the Mexican Fold-Thrust Belt and the inverted Border Rift Belt and a paleo-Rio Grande routing system north of the inverted Border Rift Belt. The paleo-Rio Grande routing system navigated evolving orogenic topography in N Mexico and the SW USA Laramide province to deliver sediment to S Texas and NE Mexico. We combine detrital zircon (DZ) U-Pb-He double dating from Late Cretaceous-Eocene strata from W Texas (Big Bend National Park) and S Texas (Eagle Pass to Laredo) along an up-to-down-dip source-to-sink depositional profile to systematically investigate sediment source exhumation, sediment dispersal, the interplay between axial and transverse sediment input, and regional drainage segregation during peripheral Laramide/Mexican orogenesis and inversion tectonics.
Depth-profiled DZ U-Pb analyses yielded dominant <85 Ma age modes that derive from Laramide and younger magmatism and 180-85 Ma age modes from various Cordilleran arcs. DZ age spectra also display subordinate Permian (Big Bend only), early Paleozoic, Neoproterozoic, 1250-950 Ma, and 1.8-1.4 Ga (more prominent in S Texas) age modes. DZ spectra also show 180-140 Ma—85-60 Ma and 1.8-1.4 Ga—85-60 Ma core-rim pairs consistent with Laramide magmas intruding the Nazas arc and Yavapai-Mazatzal crust, whereas 1.2-0.9 Ga—650-380 Ma core-rim pairs were originally sourced from the Coahuila block of north-central Mexico and subsequently recycled out of the inverted N Mexico Border Rift basins. DZ U-Pb-He double dates on 100-50 Ma U-Pb age zircons yielded 90-40 Ma (U-Th)/He dates that demonstrate unroofing of plutonic roots of the Laramide and Cordilleran arc magmatic rocks and suggest rapid tectonic unroofing of the Laramide magmatic province. Additional 255-240 Ma He double dates on 500-400 Ma U-Pb ages record heating of peri-Gondwanan zircons where the Cordilleran-East Mexico arc system crossed the Coahuila terrane; these grains were subsequently recycled from adjacent inverted rift basins.
Depth-profiled DZ U-Pb-He data demonstrate that W and S Texas strata were sourced by Laramide magmatic provinces, Cordilleran arc sources, recycled sedimentary sources in the inverted Border Rift (Chihuahua and Sabinas Basins), and Laramide basement block uplifts. Importantly, they lack DZ ages derived from the Early Cretaceous Alisitos arc which argues against sediment derivation from W Mexico and input via the Parras-La Popa routing system. These data demonstrate that the inversion of the Chihuahua-Sabinas basins segregated the paleo-Rio Grande system from the Mexican foreland, while both inputting sediment transversely and guiding sediment axially to S Texas and NW GOM. This interpreted catchment area is extensive, incorporating large portions of the SW USA and NE Mexico where it drained an evolving, tectonically active hinterland that underwent rapid Paleogene tectonic unroofing and was a major sediment source to S Texas.

Keywords: Detrital Zircon U-Pb-He Double Dating, Sediment Routing, Inversion Tectonics, Laramide Orogen, Mexican Foreland, Border Rift Belt

LCPHD-22

SETP
LCPHD

Kinematic development and structural architecture of the southern Central Andean fold-thrust belt (31?33°S): implications for Andean deformation modes and driving mechanisms

Chelsea Mackaman-Lofland
Mackaman-Lofland, C., University of Texas
Horton, B., University of Texas
Fuentes, F., YPF
Constensius, K., University of Arizona
Ketcham, R., University of Texas
Stockli, D., University of Texas
Ammirati, J., Universidad de Chile
Capaldi, T., University of Nevada Las Vegas
Orozco, P., Universidad Nacional de San Juan
Alvarado, P., Universidad Nacional de San Juan

Andean deformation above the Argentina-Chile flat-slab segment (31–33°S) has been variably attributed to flattening of the subducted Nazca plate, maintenance of thrust belt critical wedge taper, or inversion of inherited rift structures. Conflicting interpretations of deep crustal geometries—including detachment depths for basement-involved structures, location and connectivity of footwall ramps and flats, and even orogenic vergence—have further been proposed. We present new structural interpretations and thermochronological data for the hinterland Frontal Cordillera and flanking Precordillera thrust belt and foreland basin system that provide insights into the timing, geometry, and kinematics of deformation and facilitate interrogation of the potential driving mechanisms. Neogene shortening in the Frontal Cordillera was largely influenced by the inversion of Permian-Triassic extensional structures, which produced a series of broad wavelength (~10–20 km), mechanical basement-cored anticlines exhumed along west-dipping reverse faults. Reactivated basement structures transferred slip to the thin-skinned Precordillera imbricate system along a non-emergent footwall ramp beneath the easternmost basement-cored range. Hinterland structural relationships, foreland basin provenance, and apatite (U-Th)/He thermochronology results indicate sequential reactivation along Frontal Cordillera and potentially western Precordillera faults from ~24 to 14 Ma, followed by regionally synchronous thin- and thick-skinned shortening by ~12–9 Ma. Preliminary apatite (U-Th)/He cooling ages from a strike-parallel transect along the eastern Frontal Cordillera confirm mid-Miocene rapid exhumation spanned 29–33°S, refuting interpretations that deformation advanced southward during progressive flattening of the oceanic plate. Finally, late Miocene-Pliocene (~2–8 Ma) cooling ages along the eastern Frontal Cordillera and Chile-Argentina border reflect passive hinterland exhumation, potentially associated with coeval east-vergent deformation.

Keywords: Andes, convergent margins, orogenesis, foreland basin, geochronology, thermochronology

LCPHD-23

SETP
LCPHD

Unraveling the pre-subduction stratigraphy and tectonometamorphic evolution of the Internal Betics using zircon U-Pb and trace elements geochronology

Eirini Poulaki
POULAKI, E., The University of Texas at Austin, Austin, TX
STOCKLI, D., The University of Texas at Austin, Austin, TX

One of the most remarkable High Pressure/Low Temperature (HP/LT) remnant subduction zone complexes is the Nevado-Filábride Complex (NFC) and Alpujárride Complex (AC) in Southern Spain. The NFC and AC formed along the Paleozoic to Mesozoic Tethyan passive margin that was subsequently subducted, metamorphosed, and exhumed to the surface. Geodynamic models of subduction zones show that imbrication and overthrust relationships of subducted sediments should be expected. However, the NFC's and AC's complicated metamorphic history and lack of detailed geochronologic work have hampered our understanding of the paleogeography, timing of pre-subduction stratigraphy, and structural and stratigraphic correlations. In this study, we present results of U-Pb and trace elements (TE) analyses of zircon from the NFC and AC to determine the (1) provenance and paleogeography of the units, (2) initial stratigraphic arrangement and structural modifications during subduction and exhumation, and (3) the timing of metamorphism.

We collected 120 samples from all units within the NFC and the lower part of AC at various structural levels along transects perpendicular to the main foliation (N-S). We utilize novel depth-profiling techniques that ablate unpolished zircon grains from the metamorphic rims to the magmatic cores to simultaneously analyze zircon U-Pb and TE concentrations. Together, these data are used to elucidate the detrital zircon (DZ) record, Maximum Depositional Ages (MDAs), and spatial variations of geochemical signatures from the metamorphic rims to the magmatic cores. Integrating these results with structural field observations provides an unprecedented view of these complicated rocks and allows us to comprehend their complete evolution from deposition to subduction and final exhumation.

Preliminary results from NFC and AC reveal spatial and temporal variation in the DZ spectra ranging from Precambrian to Jurassic with age modes recording the evolution of these units from the Variscan orogeny to continental rifting and breakup of Pangea. We find the lower NFC consists of a thick (~4 km) Carboniferous metasedimentary succession that is homogenous both lithologically and geochronologically and may behave structurally as basement rock with no apparent modifications to the initial stratigraphy. In contrast, the uppermost NFC is significantly thinner and contains an old-over-young succession, with Permian rocks structurally above Triassic rocks. Several repetitions of AC units were also identified in the field. Together, the MDA reversals and field observations indicate thrust relationships that have modified the initial stratigraphy of the upper NFC and AC. We suggest these imbrications most likely formed during subduction. Analyses of zircon overgrowths show two distinct Cenozoic metamorphic events separated by ~15 million years with different TE signatures, which reflect the P-T conditions taking place during subduction and exhumation, respectively. This study presents a novel approach utilizing DZ U-Pb dating and field work analyses in HP/LT metamorphic assemblages, pivotal to future field studies investigating subduction processes from the geologic record.

Keywords: subduction zone, metamorphism, zircon U-Pb geochronology, stratigraphy, provenance, Southern Spain, Alboran domain

SETP
LCPHD

Geochronologic Constraints on Carboniferous Arc Magmatism in the Chicxulub Impact Crater

Catherine Ross
Ross, C., Jackson School of Geosciences, University of Texas at Austin, Austin, TX
Stockli, D., Jackson School of Geosciences, University of Texas at Austin, Austin, TX
Rasmussen, C., University of Texas Institute for Geophysics, University of Texas at Austin, Austin, TX
Gulick, S., University of Texas Institute for Geophysics, University of Texas at Austin, Austin, TX
de Graaff, S., Vrije Universiteit Brussel, Belgium
Claeys, P., Vrije Universiteit Brussel, Belgium
Pickersgill, A., University of Glasgow, Glasgow, U.K
Kring, D., Lunar and Planetary Institute -USRA, Houston, TX
Wittmann, A., Arizona State University Tempe, AZ
Schiemder, M., Lunar and Planetary Institute -USRA, Houston, TX

Determining the nature and age of the Chicxulub target rock is an essential step in advancing the understanding of the Pre-Mesozoic history of Yucatán basement, K-Pg ejecta signatures, and character of the impact-induced hydrothermal system. As few age constraints exist for the northern Yucatán basement underlying the Chicxulub crater, the IODP-ICDP Expedition 364 drillcore provides a unique opportunity to illuminate the pre-impact tectonic evolution of the Yucatán block. While the sparse record of Yucatán basement points to Pan-African and peri-Gondwanan crust (~540-550 and 450 Myr, respectively), these ages are consistent with plate reconstruction models. However, granitic zircon grains recovered from the IODP Exp. 364 peak ring drillcore exhibit U-Pb ages between 320 and 345 Ma (n=607). Ce and Eu anomalies, Th-U ratios, and proportions of heavy rare earth elements (REE) to light REE reveal a continental arc setting for the formation of the granitoids. Inherited zircon ages fall in three clusters from 400-435 Ma, 500-635 Ma, and 940-1400 Ma. The inherited ages are consistent with Peri-Gondwanan, Pan-African continental arcs, and Oaxaquian juvenile crust, respectively. The trace element compositions, Carboniferous U-Pb ages, and inherited ages indicate a pre-collisional continental arc located along the northern margin of the Yucatán before northwest Gondwana collided with Laurentia. Evidence from the granite samples establishes the southward subduction of the Rheic Ocean beneath the Yucatán. Similar evidence of a continental arc within Peri-Gondwanan terranes along the northern margin of Gondwana is documented in the Coahuila terrane of northeastern Mexico, the Suwannee terrane (Florida), and the Sabine block. Distal K-Pg deposits host Pan-African ages; however, ejecta from Saskatchewan and Colorado yield a minor component of zircon ages in the Carboniferous. While these zircon grains were commonly discarded or disregarded as suffering from lead loss, the peak ring granitoids from within the Chicxulub crater verifies the tectonic source for Carboniferous ages within K-Pg boundary sites. New zircon U-Pb ages and trace element analyses from the peak ring granitoids provide new constraints on the continental arc magmatism along the northern margin of the Yucatán in the Carboniferous and as well as a new age to trace within K-Pg boundary deposits.

Keywords: continental arc magmatism, Yucatan basement, Chicxulub impact structure, zircon U-Pb geochronology, Rheic ocean closure

LCPHD-25

SETP
LCPHD

Strike-Slip Enables Subduction Initiation Beneath a Failed Rift: New Seismic Constraints from Puysegur Margin, New Zealand

Brandon Shuck
Shuck, B., The University of Texas at Austin
Gulick, S., The University of Texas at Austin
Van Avendonk, H., The University of Texas at Austin
Gurnis, M., California Institute of Technology
Sutherland, R., Victoria University of Wellington
Patel, J., Victoria University of Wellington
Hightower, E., California Institute of Technology
Saustrup, S., The University of Texas at Austin
Hess, T., The University of Texas at Austin
Stock, J., California Institute of Technology

The critical ingredients and conditions to initiate a new subduction zone are widely debated. However, there is general agreement that subduction initiation likely takes advantage of previously weakened lithosphere and may prefer to nucleate along pre-existing plate boundaries. To evaluate how past tectonic regimes and lithospheric structures might facilitate underthrusting and lead to a mature convergent setting, we present an analysis of the Puysegur Margin, a young subduction zone with a rapidly evolving tectonic history.

The Puysegur Margin, south of New Zealand, currently accommodates convergence between the Australian and Pacific plates while exhibiting an active seismic Benioff zone, a deep ocean trench, and young adakitic volcanism in the overriding plate. Tectonic plate reconstructions show that the margin experienced a complicated transformation from rifting to seafloor spreading, to strike-slip motion, and most recently to incipient subduction, all in the last ~45 million years. However, details of this tectonic record remained incomplete due to the lack of high-quality seismic data throughout the margin.

Here we present seismic images from the South Island Subduction Initiation Experiment (SISIE) which surveyed the Puysegur region in February-March, 2018. SISIE acquired 1252 km of deep-penetrating multichannel seismic (MCS) data on 7 transects, including 2 regional dip lines coincident with Ocean Bottom Seismometers (OBS) deployments which extend (west to east) from the incoming Australian plate, across the Puysegur Trench and Puysegur Ridge, over the Solander Basin and onto the continental Campbell Plateau passive margin.

We integrate pre-stack depth migrated MCS profiles with OBS tomography models to constrain the tectonic development of the Puysegur Margin. Based on our results we propose the following Cenozoic evolution: (1) The entire Solander Basin contains thinned continental crust which formed from orthogonal stretching between the Campbell and Challenger plateaus during the Eocene-Oligocene. This phase of rifting was more pronounced to the south, producing thinner crust with abundant syn-rift volcanism across a wider rift-basin, in contrast to the relatively thicker crust, moderate syn-rift volcanism and narrower rift basin in the north. (2) Following, strike-slip deformation developed atop Puysegur Ridge, completely outside the locus of rifting and within relatively unstretched continental lithosphere. This proto strike-slip plate boundary translated unstretched crust northward causing a continent-collision zone, which led to a transpressional pattern of distributed left-stepping faults. (3) Subduction initiation was aided by large density contrasts as oceanic lithosphere translated from the south forcibly underthrusted the continent-collision zone. The early development of oblique subduction generated modest and widespread reactivation of faults in the upper plate. (4) At present-day, the Puysegur Trench shows a temporal transition from nearly mature subduction in the north to a younger initiation stage along the southernmost margin.

Our new seismic images suggest subduction initiation at the Puysegur Margin was assisted by inherited buoyancy contrasts and structural weaknesses that were imprinted into the lithosphere during earlier phases of continental rifting and strike-slip along the developing plate boundary. The Puysegur Margin demonstrates that forced nucleation along a strike-slip boundary is a viable subduction initiation model and should be considered throughout Earth's history.

Keywords: subduction initiation; continental rifting; strike-slip tectonics; seismic imaging

SETP
LCPHD

Upper Mantle Dynamics And Seismic Anisotropy From Synthetic Waveforms

Wanying Wang
Wang, W., Institute for Geophysics and Department of Geological Sciences, The University of Texas at Austin
Becker, T., Institute for Geophysics and Department of Geological Sciences, The University of Texas at Austin

Seismic anisotropy is a constraint for mantle dynamics and thus important in studying the upper mantle. In our previous work on North American continental dynamics, we used mantle flow models to predict seismic anisotropy in light of shear wave splitting (SWS) results. We verified the validity of our flow models and established a new methodology to study the extent of frozen-in anisotropy within the lithosphere. However, with the 1-D approximation of sublithospheric anisotropy in our previous study, it is hard to fully exploit the constraints provided by SWS, especially how they integrate the depth varying seismic anisotropy. For this, we extend our work by modeling global seismic wave propagation, while accounting for the 3-D heterogeneity of mantle flow predicted anisotropic elasticity tensors. We use AxiSEM3D, which is a spectral element method, and a dimension reduction algorithm to conduct fast, full waveform propagation computations. Our waveform modeling is largely based on our understanding of the Earth through seismic tomography, which is consistent with our mantle flow modeling approach. In the lithosphere, we use the LITHO1.0 velocity model, and test for the lithospheric anisotropy by including the hypothetical lithospheric tensors from our previous work. We verify the validity of these model settings by confirming the overall similarities between the resulted waveforms to the reference waveforms computed from the PREM model. We are currently in the process of conducting SWS analysis for specific stations using the synthetic seismograms, and repeating this process for multiple seismic events for a full back-azimuthal coverage. This approach might also bring insight to understand the very limited correlation between anisotropy from SWS and that from surface waves, which has been observed in previous studies and is further confirmed in our tests with the updated SWS dataset. The lack of correlation might be partly due to the difference in resolution, but there might be other contributions. We explore this problem by computing synthetic surface wave phase velocity anomalies and azimuthal anisotropy to examine their correlation with the corresponding SWS parameters for different model settings.

Keywords: Lithosphere, asthenosphere, seismic anisotropy

SHP
LCPHD

Fluid residence time modules Li isotope transport during silicate weathering

Evan Ramos
Ramos, E., Department of Geological Sciences, The University of Texas at Austin, Austin, TX
Capaldi, T., Department of Geological Sciences, The University of Texas at Austin, Austin, TX; Department of Geosciences, Utah State University, Logan, UT
Sickmann, Z., Department of Geological Sciences, The University of Texas at Austin, Austin, TX; University of Texas Institute for Geophysics, The University of Texas at Austin, Austin, TX

The Li isotope composition of river water is used as a direct tracer of the intensity of silicate weathering throughout a drainage catchment. In this context, weathering intensity is best considered as the degree to which the products of primary weathering form secondary minerals, especially clays. Understanding what governs silicate weathering intensity and how it has changed through geologic time informs our understanding of the carbon cycle, planetary habitability, and the evolution of biogeochemical cycles on Earth. Chemical weathering is often cast in terms of mineral and fluid residence time to enable a mechanistic understanding of weathering-sensitive geochemical proxies. While mineral residence time has been considered in the interpretation of Li isotope river water chemistry, principles of fluid residence time (FRT) have largely remained unexplored.

To interrogate the relationship between FRT and Li isotope river water chemistry, we take a twofold approach. First, we develop a two-dimensional (2D) reactive transport model for Li isotopes to predict river δ^7Li values as a function of FRT. In our model, we compute steady-state river water δ^7Li values over a range of crustal permeabilities, primary mineral dissolution rates, aquifer thicknesses, reaction stoichiometries, and catchment-average hillslopes. Simulations comparing FRT with river water δ^7Li values exhibit three key trends: (1) when FRT is high (> 5 years), clay mineral formation overwhelming influences river water δ^7Li values; (2) when FRT is low (< 6 months), clay mineral formation is subdued and river water δ^7Li values approach primary/bedrock mineral δ^7Li values; (3) at intermediate FRTs, predicted river water δ^7Li values reach maxima due to Rayleigh fractionation of Li isotopes. The magnitudes of maximum δ^7Li values are a function of reaction stoichiometry whereas the FRTs at which the maxima occur depend upon the relative rates of clay mineral precipitation and fluid advection.

We then amass a global dataset of published river water δ^7Li values and determine the morphometric, climatological, and lithologic properties of their drainage catchments. Kernel density estimates and statistical surveys of the data show that a combination of drainage catchment property must be used to explain the range of river water δ^7Li values. Through Darcy's Law, we synthesize catchment properties to predict an average FRT for each river water sample. Notably, our model FRT predictions are comparable to those gleaned from the global dataset, suggesting that FRT is a primary influence on the Li isotope chemistry of rivers worldwide. Our findings underscore the inextricable link between the hydrologic cycle and the geologic carbon cycle.

Keywords: silicate weathering, Li isotopes, carbon cycle, fluid residence time, hydrology

SHP
LCPHD

Direct measurements of water storage in unsaturated rock

Logan Schmidt
Schmidt, L., The University of Texas at Austin, Austin, TX
Rempe, D., The University of Texas at Austin, Austin, TX

Water content in the unsaturated bedrock weathering profile is a very important geophysical parameter to accurately measure as it can be used to compute fluxes of water, solutes and gas to drive models of critical biogeochemical processes in the deep vadose zone. However, due to technological and logistical constraints, there are few available or established methods for obtaining direct measurements of hydrologic processes in the complex subsurface environment. In this field study, we present estimates of key hydrologic parameters---water content and storage---in the unsaturated weathering profile underlying two intensively monitored hill slopes derived from direct borehole measurements using a nuclear magnetic resonance (NMR) tool and a neutron moderation (neutron) probe. During a summer dry growing season, we obtained successive well logs with both methods in a network of boreholes at two sites associated with the Eel River Critical Zone Observatory. We used sets of repeat measurements were obtained with both tools to estimate uncertainty. We find that, with the specific acquisition parameters used in this study, neutron estimates of water content are more precise than NMR measurements, but water content is detectable by both methods even in the driest conditions. We compare paired NMR and neutron estimates of water content and show that both methods detect the same water content change and estimates of dynamic water storage derived from each method agree. This agreement suggests that both methods are robustly sensitive to water content and not other temporally variable conditions in the bedrock weathering profile. Finally, we demonstrate that, with acquisition parameters tuned to accommodate the measurement challenges presented by the unsaturated bedrock environment, the precision of NMR measurements can be significantly improved.

Keywords: vadose, hydrology, geophysics, NMR, neutron, unsaturated, ecohydrology

SHP
LCPHD

Considering unsaturated bedrock in global carbon cycling: CO2 production and DOC dynamics in weathered bedrock in a forested hillslope

Alison Tune
Tune, A., Dept. of Geological Sciences, Jackson School of Geosciences, University of Texas at Austin
Druhan, J., Dept. Of Geology, University of Illinois at Urbana Champaign
Wang, J., Dept. Of Geology, University of Illinois at Urbana Champaign
Bennett, P., Dept. of Geological Sciences, Jackson School of Geosciences, University of Texas at Austin
Rempe, D., Dept. of Geological Sciences, Jackson School of Geosciences, University of Texas at Austin

In many upland ecosystems, thin soils are underlain by fractured and weathered bedrock. In these thin soiled hillslopes, roots and the rhizosphere extend into bedrock to access water and nutrients, producing organic carbon in the process. Carbon-hosting sedimentary rocks, such as carbon-rich mudstones, may provide an additional source of organic carbon in upland ecosystems. This organic carbon can be advected to groundwater or degraded in-situ, and the resulting CO_2 can be diffused out of the subsurface towards the atmosphere, dissolved into water, chemically weather rock, and or be exported in ground and streamwater. Yet we do not know how significant these processes are in weathered bedrock systems for carbon cycling both within individual ecosystems and to the global carbon cycle. It is difficult to constrain the effect of deep rooting and lithology, and incorporate these processes into models, because it is challenging to sample water and gas in unsaturated, weathered rock, and as a result, few datasets exist. Here we present two years of data collected at the Eel River Critical Zone Observatory in a novel vadose zone monitoring system (VMS) that samples water and gas over a 16 m thick, variably saturated argillite weathering profile. We find significant CO_2 production and export meters beneath thin soils, leading us to ask: what sources of organic carbon are respired in weathered bedrock? We present data on dissolved organic compounds, including characterization through column chromatography and spectroscopy. We find high concentrations of dissolved organic carbon (DOC) throughout the weathered bedrock unsaturated zone. While CO_2 concentrations have a clear vertical and temporal structure, DOC concentrations are more variable over time. Our CO_2 and DOC analyses indicate carbon cycling in unsaturated, weathered bedrock is important in ecosystems where deep roots are present.

Keywords: carbon cycling, carbon dioxide, critical zone, bedrock

SHP
LCPHD

Bedforms of a Supercritical Fan

Logan West
West, L., Dept. of Geosciences, The University of Texas at Austin, Austin, TX

Numerical and physical modeling as well as direct observation of turbidity currents indicates that sediment gravity flows commonly reach Froude supercritical states over moderately steep slopes. This occurrence is reflected in seafloor bathymetry data, which reveal that such flow conditions impact how and where sediments are deposited. However, the stratigraphic details of the resulting deposits, their preservation potential, and their significance in sediment transport, basin evolution, and reservoir applications remain incompletely understood. This work analyzes seismic-scale outcrop exposures in the Fish Creek-Vallecito Basin deposited along the steep margins of the early Gulf of California in south-central California. The result is a detailed three-dimensional (3D) characterization and interpreted outcrop model of an evolving supercritical fan, which is used to describe the architecture of supercritical bedforms and spatiotemporal evolution of the deposits as well as provide first order constraints on the depositing flow conditions.

Keywords: Deepwater, Supercritical, Bedform, Antidune, Cyclic Step, Hydraulic Jump, Salton Trough, Gulf of California

U

Provenance and Commercial Significance of Industrial Stonework Lithologies from 3rd Century Ruins of Volubilis, Morocco

Lauren Lobue
LoBue, L., Department of Geological Sciences, The University of Texas at Austin, Austin, TX
Culotta, S., Department of Geological Sciences, The University of Texas at Austin, Austin, TX
Bittner, M., Department of Geological Sciences, The University of Texas at Austin, Austin, TX
Benton, J., Department of Art, Old Dominion University, Norfolk, VA
Schirmer, C., Department of Classics, The University of Texas at Austin, Austin, TX
Walthall, A., Department of Classics, The University of Texas at Austin, Austin, TX
Orlandini, O., Department of Geological Sciences, The University of Texas at Austin, Austin, TX

The UNESCO world heritage site of Volubilis in central Morocco preserves many details of 3rd century CE Roman industry and commerce. The Urban Economy of Volubilis Project undertakes to study the economic complexity of the city by studying the professional and social methods of its craftspeople. In this work, we analyze the lithologies of industrial bakery and olive press stoneware using optical petrography, X-ray micro-analysis, and powder X-ray diffraction in order to better constrain the provenance of these tools.

We analyzed 16 millstones from Volubilis and found that the lithology of stoneware was cleanly divided by industrial application. Bread mixer/kneader lithologies are carbonates composed of mm-scale micritized ooids with scant foraminifera and other fossil fragments, suggesting a low depositional energy. Millstones from olive presses are also carbonates but show an unusually high depositional energy with abundant cm-scale mollusk and bryozoan shells. Bakery millstones are vesicular basalts, with distinct Mg-depletion rims on mafic phases and a uniform mm-scale feldspar groundmass.

The clear grouping of lithologies in the studied millstones suggests that Volubilis millstones likely derived from three different quarry sources. The lack of intermixing of lithologies between applications further suggests that each quarry source is uniquely associated with the final production of a specific type of tool. In combination with very similar design and materials within specific tools, this suggests a high degree of coordination in each industry. Although the specific source quarries for these lithologies is yet to be determined, the practice of using vesicular basalts for milling grains was common in Italy and Sicily and may indicate a Mediterranean origin for these tools.

Keywords: Petrology, Archeology, Microscopy

U

Determining an Optimal Window Size for Accurate Curie Depth Measurements

Chinmay Murthy
Murthy, C., University of Texas at Austin Institute for Geophysics, Austin, TX
Greenbaum, J., University of Texas at Austin Institute for Geophysics, Austin, TX
Young, D., University of Texas at Austin Institute for Geophysics, Austin, TX
Blankenship, D., University of Texas at Austin Institute for Geophysics, Austin, TX

Estimating geothermal heat flux (GHF) at the base of the Antarctic Ice Sheet is essential for constraining numerical ice sheet models that will predict global sea level change. One method to determine the GHF begins via estimates of the depth at which crustal rocks lose their ferromagnetism, called the Curie point depth (CPD). This method is widely applied, making use of the large spatial coverage and detail of existing magnetic datasets such as Antarctic Digital Magnetic Anomaly Project (ADMAP). The centroid spectral method has been extensively used to estimate the CPD for regional magnetic anomalies, wherein a radial power spectrum of magnetic data is analyzed over a certain window size. The depths to the top of the magnetic source and the centroid of the source are then estimated using scaled slopes of the power spectrum at higher and lower wavenumbers, respectively. However, the magnitudes of the slopes are related to the window size where, for small windows, shorter wavelengths and higher wavenumbers of the magnetic data could be filtered out. Furthermore, the centroid spectral method is based on the assumption that the magnetic source is parallelepiped shaped, with its length and width much larger than its depth.

Here we determine an optimal window size for the power spectrum to estimate the CPD using ADMAP data. We use windows of various sizes and calculate the power spectrum of the magnetic data for each window. Using the centroid spectral method as per Tanaka et al. (1999), Li et al. (2009), we then derive estimates of the top and centroid of the magnetic source for each window size and apply a best fit a modelling approach using a random magnetization model to derive the most accurate CPD.

Results from this research will help in evaluating the accuracy of CPDs in Antarctica, which can improve estimates of the GHF over ice covered regions. This will provide boundary conditions for models of ice sheet evolution. Furthermore, this research will improve the detection of thin-crust areas, thus allowing for better detection of rift zones and other tectonic features that are crucial in reconstructing the geological history of Antarctica.

Keywords: Magnetics, Geomagnetism, Curie point depth

CCG
U

Biotic Influence on Speleothem Morphology

Carole Lakrout
Lakrout, C., Jackson School of Geosciences, University of Texas at Austin, Austin, TX
Goldfarb, E., Jackson School of Geosciences, University of Texas at Austin, Austin, TX
Bontognali, T., Space Exploration Institute Environmental Science Center; Qatar University. Department of Environmental Sciences; University of Basel,
Tisato, N., Jackson School of Geosciences, University of Texas at Austin, Austin, TX

Studying life in harsh conditions can provide information about habitability in our and other planets. One example of such a harsh environment is a cave in France (Asperge), which contains mineral deposits called helictites that grow in a room with little water, no light, and a heavy concentration of metals in the rocks.

Two helictites morphologies were found in Asperge: acicular and tubular. The former is aragonite and has a central micro-tube. The latter is calcite and has a large central hole. The Asperge helictites were analyzed by Tisato et al. (2015) who proposed that the formation of tubular concretions is orchestrated by life. However, still relatively little is known.

Similar speleothems have been observed in a cave in Colorado (Breezeway). A common nature for both the Breezeway and Asperge speleothems would provide a strong argument for the bio-mediated formation of such helictites. Here, we report analyses on speleothems from Breezeway.

Breezeway has less water than Asperge, no light, and the helictites appear to grow on a paleo-laterite soil. In-situ observations reveal the presence of millimetric white dots covering the walls of the cave and speleothems. These white dots have been identified as bio colonies found only near the helictites and resemble those found in Asperge. Due to the morphological similarity and the presence of the white dots, we hypothesize that like the speleothems in Asperge, the mineral deposits from Breezeway have formed biotically. We can prove this by examining high resolution images for biotic films, textures, and chemical elements.

We performed the following analyses on five samples: X-ray diffraction to study mineralogy of the speleothems; Micro-CT to study morphologies of speleothems; Scanning Electron Microscopy to investigate the presence of biofilms; and SEM Energy Dispersive Scanning to analyze the mineralogy of specific micrometric volumes of the samples.

The large hole in the tubular concretions suggests that tubular concretions formed biotically. We also observe that calcite crystals of tubular concretions are covered by a “low-density” layer. Such a layer is tens of microns in thickness and was further investigated with SEM imaging.

SEM imaging of tubular samples reveals the presence of biofilms and mineral structures likely related to biological activity. Using the SEM images, we interpret calcite “construction-sites” covering calcite crystals as minerals in the process of growing by the addition of calcite flakes. Small filaments create bridges between the calcite “flakes” and the calcite crystal. These filaments are biomass and a remnant of microbial life activity. Some evidence of biological activity on acicular speleothems were also collected. On a couple of acicular samples, we biomass. This suggests that originally abiotic acicular speleothems are colonized by microbial life.

This research furthers the understanding that life exists in extreme environments. Understanding how life can thrive in these conditions is a starting point for the study of life on our and other planets. Given that caves are present on Mars and other planetary bodies, we suggest a potential way to search for past or present evidence

of life in the geological record.

Keywords: geomicrobiology, speleothem, helictites, caves, biologically mediated

EG
U

Cementation of Solution-Collapse Breccias in the Lower Ordovician Upper Knox Group, Central Tennessee

Thomas Quintero
Quintero, T., Department of Geological Sciences, The University of Texas at Austin, Austin, TX
Kyle, J., Department of Geological Sciences, Bureau of Economic Geology, The University of Texas at Austin, Austin, TX
Miller, N., Department of Geological Sciences, The University of Texas at Austin, Austin, TX
Ukar, E., Bureau of Economic Geology, The University of Texas at Austin, Austin, TX

The central Tennessee-southern Kentucky region features active zinc mines with ore hosted in the Lower Ordovician Upper Knox Group carbonate breccias. These breccia systems also form local oil reservoirs in this region, as well as in the deep Permian Basin in West Texas as part of the “Great American Carbonate Bank” which extends across the continental United States. The porosity in these extensive breccia systems commonly is partially occluded by carbonate cements while lacking Mississippi Valley-Type (MVT) lead-zinc ore, indicating the need for a greater understanding of the relationship between brecciation and local MVT mineralization. The deposition of these cements also reduces porosity and permeability, inhibit fluid migration pathways, and decrease reservoir storage capacity emphasizing the need to study the extent, timing and characterization of dissolution and mineral cement precipitation. The sequence of cementation in the solution-collapse breccias is defined using the physical and chemical properties of the mineral cements.

Exploration cores and mining exposures provide extensive three-dimensional information about the breccia systems. Systematic logging and sampling of continuous exploration cores from above the Knox unconformity through the Upper Knox Group allows breccia and cement distribution to be documented over ~300-m of stratigraphic section. The mineral cement paragenesis and chemistry are being studied using a combination of petrography, optical cathodoluminescence (CL) zonation imaging, LA-ICP-MS trace element analysis, high resolution X-ray computed tomography (HRXCT), and scanning electron microscope (SEM)-based CL.

As in previous Knox cement studies, CL imaging has revealed microstratigraphic zones in dolomite and calcite cements. Geochemical analysis via LA-ICP-MS is being used to assess variation in the trace element concentrations in the carbonate cements with an objective of defining multiple stages, including ore-forming events. The 3-D distribution of compositionally contrasting carbonate zones, such as Fe-rich dolomite zones, and their association with ore minerals can be mapped using HRXCT. SEM-CL provides high-resolution, large-area mapping capability to detect compositional variations that can be correlated regionally.

Results indicate initial silicification of dolostone and quartz cementation of breccia, followed by multiple stages of calcite and dolomite, in association with local pyrite, sphalerite, galena, fluorite, and barite cements. Seven interpreted dolomite zones differ qualitatively in their luminescence and color as well as quantitatively among the concentration of trace elements such as Fe, Mn, Zn, Sr, Ba, La, and Ce. Trace element data of dolomite cements can allow for a more accurate correlation of dolomite cement zones across significant distances. HRXCT scans reveal a highly attenuating zone inside of dolomite crystals which could correlate to the Fe-rich D-4 dolomite zone. Pyrite is scattered throughout the younger low-Fe cement indicating that sulfide precipitation controls the Fe content of dolomite cement. These results could improve mineral exploration strategies by providing a guide for temporal and spatial controls for local MVT mineral deposition.

Keywords: economic geology, carbonate, cement, zonation, laser, ablation, cathodoluminescence, computed tomography

MG
U

Holocene Sea Level Rise and Paleo-environmental Change within Trinity River Paleo-valley Offshore Galveston Bay, Gulf of Mexico

Patricia Standring
Standring, P., Jackson School of Geosciences, University of Texas
Lowery, C., Institute for Geophysics, University of Texas
Gulick, S., Institute for Geophysics, University of Texas
Swartz, J., Institute for Geophysics, University of Texas
Goff, J., Institute for Geophysics, University of Texas

As the Texas Gulf Coast becomes more vulnerable to sea level rise, it is increasingly important to constrain the response of different parts of the coastal environment to this forcing. Differing effects are expected due to variable rates of sediment supply and subsidence. Paleo records can augment historical data to determine long-term sea level histories of the Texas shelf. Just as the modern Trinity River empties into Galveston Bay, offshore beneath the modern seafloor lies the Trinity River paleo-valley and overlying paleo-estuarine fill which record sea level rise following the Last Glacial Maximum. In addition to a record of the marine transgression, the paleo-river valley contains fluvial sand deposits (e.g., point bars) which represent a crucial resource on the sand-poor Texas shelf and may be used for coastal rejuvenation projects. Here, we present paleo-environmental data from biostratigraphic analysis of sediment cores from the Trinity River paleo-valley to provide a more complete reconstruction of the former river valley. Carbon-dated macrofauna found in the sediment cores provide exact timing on relative sea level rise and place these cored depths in context. Geophysical (chirp) survey data image sedimentary strata which record the evolution of the Texas shelf during the Holocene transgression. Sedimentary and benthic foraminifera analysis of piston cores reveal a rise in sea level and a change in the paleo-environment from fluvial to estuarine over a several kyrs. Our data indicate the development of an estuary offshore of the modern Galveston Bay as early as 8,600 ± 30 calendar years before present (CBP). The estuary transitioned to an outer bay environment by 7,690 ± 25 CBP as sea levels continued to rise. Samples shift between the predominance of the genera *Ammonia* (indicating a middle bay environment) and *Elphidium* (indicating an outer bay environment), within low diversity assemblages, which indicates an estuarine environment filled the paleo-valley that shifted from middle to outer bay. These data indicate fluctuations in relative sea level and/or salinity, but overall also imply long-term stability of an estuarine environment during the late Holocene. The presence of probable washover deposits in multiple cores indicate this paleo-estuary was likely protected by a barrier system before being overcome by sea level rise. Outer bay facies are overlain by the modern seafloor, less than 20 km offshore, indicating either rapid sea level rise or a sudden shift in sediment supply terminated the paleo-estuary.

Keywords: Foraminifera, Galveston Bay, Holocene, Sea Level Change

SETP
U

DETRITAL ZIRCON U-PB DATA FOR PENNSYLVANIAN SANDSTONES FROM THE EASTERN SHELF OF THE PERMIAN BASIN - INSIGHTS INTO SYN-COLLISIONAL OUACHITA SEDIMENT PROVENANCE AND SEDIMENT ROUTING SYSTEMS

Thomas Ditges
Ditges, T., Jackson School of Geosciences, The University of Texas at Austin, Austin, TX
Standring, P., Jackson School of Geosciences, Institute for Geophysics, University of Texas at Austin, Austin, TX
Stockli, D., Department of Geological Sciences, Jackson School of Geosciences, The University of Texas at Austin, Austin, TX

The Fort Worth and Permian Basins of central and southwest Texas are part of the Ouachita flexural foreland basin that developed along the southern margin of Laurentia in late Paleozoic times. Significant uncertainty surrounds sediment provenance of Pennsylvanian syn-orogenic strata, paleo-drainage evolution, and sediment routing system during progressive Ouachita collision. In particular, the existence of an Alleghanian axial drainage system versus a transverse sediment delivery system from the Ouachita orogenic belt and Gondwana hinterland remains debated. This study presents new zircon U-Pb data from sandstone samples from the Eastern Shelf of the Permian Basin, spanning Atokan Smithwick, Desmoinesian Strawn, and Virgilian Lower Cisco sandstones exposed along the NW margin of the Precambrian Llano Uplift. The data exhibit consistent detrital zircon U-Pb spectra dominated by Grenville and late Neoproterozoic, and minor Carboniferous, Ordovician, Cambrian, Meso- and Paleoproterozoic, and Archean age components. The observed DZ U-Pb signatures are in stark contrast to typical Alleghanian spectra, dominated by >1 Ga and Ordovician zircon ages, strongly arguing against major input via a regional axial sediment routing system. In particular, the presence of 320-350 Ma zircons, likely sourced from the pre-collisional magmatic arc, prominent Neoproterozoic, and 930 Ma age peaks imply sourcing from the Ouachita hinterland and tapping into Gondwana and Oaxaquian source terranes and therefore a transverse syn-collisional sediment routing system. Interestingly, the age-equivalent Pennsylvanian Haymond Fm. in the Marathon area shows identical DZ U-Pb signatures, suggesting a possible axial connection to the Eastern Shelf or tapping into similar orogenic hinterland source terranes. Up-section in the Lower Cisco Group exhibits more Cambrian DZ ages pointing to possible a linkage to northern source in the S Oklahoma aulacogen. In summary, the consistent and cosmopolitan detrital zircon U-Pb age signatures of Pennsylvanian syn-orogenic strata in central Texas argue for a persistent and dominant sediment delivery system to the southeastern Permian Basin via the Eastern Shelf directly from the Gondwanan orogenic hinterland as well as a possible axial linkage the incipient Marathon foreland basin.

Keywords: Detrital zircon, geochronology, Pennsylvanian, Eastern Shelf, Permian Basin

SETP
U

STRATIGRAPHIC ARCHITECTURE AND PROVENANCE OF THE CRETACEOUS CERRO BARCINO FORMATION, PATAGONIAN BROKEN FORELAND BASIN, SOUTHERN ARGENTINA

Anthony Edgington
Edgington, A., Department of Geological Sciences, Jackson School of Geosciences, The University of Texas at Austin, Austin, TX
Butler, K., Department of Geological Sciences, Jackson School of Geosciences, The University of Texas at Austin, Austin, TX
Horton, B., Institute for Geophysics and Department of Geological Sciences, Jackson School of Geosciences, The University of Texas at Austin, Austin, TX

The late-Early Cretaceous Las Plumas and Cerro Castaño members of the Cerro Barcino Formation comprise an anomalously coarse-grained interval within the widespread and dominantly fine-grained Cretaceous Chubut Group of the Patagonian broken foreland basin, Chubut Province, Argentina. The coarse-grained character and distal position of this stratigraphic interval may signal a change from continuous to broken foreland basin settings. To address this hypothesis, we assess the provenance and depositional history of the Las Plumas-Cerro Castaño succession. We employ a multifaceted provenance approach including detrital zircon U-Pb geochronology, conglomerate clast counts, and sandstone petrography. Detailed unit descriptions, correlated stratigraphic sections, and detrital zircon U-Pb maximum depositional ages are used to refine the regional chronostratigraphic framework. Our results indicate maximum depositional ages of 107.21 ± 0.97 Ma (Albian) for the Cerro Castaño Member and 107.6 ± 1.2 Ma (Albian) and 96.2 ± 1.5 Ma (Cenomanian) for the Las Plumas Member. Provenance results indicate a polarity reversal from a west-derived Andean sediment source (<145 Ma) during the deposition of the Cerro Castaño Member to east-derived intrabasinal basement-uplift sources (~188-172 Ma and >300 Ma) during the deposition of the Las Plumas Member. This switch in dominant detrital age population is accompanied by a change in depositional environment from fine-grained fluvial-lacustrine to conglomeratic braided fluvial conditions. We conclude this shift in sedimentary provenance signals foreland basin partitioning by basement-involved uplift during the late-Early Cretaceous.

Keywords: Andes, Patagonia, Foreland basin, Provenance, Stratigraphy, U-Pb geochronology

SHP
U

Evaluating chemical depletion as a weathering indicator in heterogeneous, sedimentary systems

Rachel Breunig
Breunig, R., Jackson School of Geosciences, The University of Texas at Austin, Austin, TX
Rempe, D., Jackson School of Geosciences, The University of Texas at Austin, Austin, TX
Pedrazas, M., Jackson School of Geosciences, The University of Texas at Austin, Austin, TX

Weathering processes generate porous and permeable soils from rock, radically changing the mobility and hydrologic dynamics of Earth's near surface critical zone. Chemical depletion is one method for evaluating the extent and spatial pattern of weathering and assessing weathering mechanisms. Elemental composition of bedrock throughout a weathering profile is typically normalized using protolith composition. Depletion or augmentation of mobile elements is determined relative to immobile elements. Therefore, interpretation of chemical depletion depends strongly on the assumption that weathered bedrock and protolith share mineralogy. In interbedded sedimentary bedrock systems, this assumption is typically violated and the extent to which chemical depletion can be used to evaluate weathering processes is unknown. Here, we present weathering profile characterization results from multiple field sites underlain by variably metamorphosed, interbedded sandstones and mudstones. We compare various metrics of weathering extent such as mineralogy, bulk density, porosity, and grain size to records of elemental composition to evaluate the extent to which measures of chemical depletion can be used in such heterogeneous systems. A large fraction of Earth's terrestrial surface is comprised of sedimentary bedrock, therefore, it is important to establish the utility and limitation of chemical weathering indices in sedimentary bedrock.

Keywords: Chemical Depletion, Weathering, Heterogeneity

SHP
U

Deducing the Timing and Magnitude of Late Quaternary Mississippi River Deltaic Progradation and Retrogradation Coeval with the Waning Phase of the Last Glacio-eustatic Cycle by Modelling Volumetric Flooding Rate and Sediment Discharge Since the Cessation of the Late Wisconsin Glacial Stage

Ryan Herring
Herring, R., Institute for Geophysics and Department of Geological Sciences, Jackson School of Geosciences, The University of Texas at Austin, Austin, Texas 78712, U.S.A.
Olariu, C., Department of Geological Sciences, Jackson School of Geosciences, The University of Texas at Austin, Austin, Texas 78712, U.S.A.
Helper, M., Department of Geological Sciences, Jackson School of Geosciences, The University of Texas at Austin, Austin, Texas 78712, U.S.A.

Attaining a better understanding of paralic sedimentary deposits is of high importance because they provide a key link to understanding sediment fate in a source-to-sink perspective. In order to achieve a greater understanding of sediment dispersal during transgression and regression associated with river deltas, the last such cycle of the Mississippi River delta is studied herein. Previously published maps and borehole data of the Mississippi valley, delta, and shelf deposits have been compiled to discern how the Mississippi locus of deposition fluctuated since the Last Glacial Maximum (LGM). Additionally presented is a model by which to determine when an ancient river system is in prograde or retrograde phase during periods of sea level fluctuation.
At the LGM (19ka) when the sea level was 120 metres below present, the Mississippi River lay entrenched into the shelf and it built its deltas on the shelf margin. As the base level rose rapidly subsequent to the LGM, the river filled its valleys with sediment in the ensuing retrogradation and formed depocentres in front of and basinward of the valley. As the sea levelled, the river's deltas prograded from the mouth of the valley outside of its valley onto the open shelf. Employing previously published data showed that shelf depocentres migrated widely, ~300 km, from the outer to the inner shelf and back again following sea level rise.
By volumetrically comparing the amount of sediment deposited over a time interval with the flooding volume, visualised as the new volume encapsulated between the surface, the sea level at t_0, and the sea level at t_1, the timing in which a river delta was undergoing progradation or retrogradation can be determined. This study posits that, from a volumetric perspective, when the flooding volume is in excess of the sediment volume deposited by a system during a given time period, then the system must undergo retrogradation. Conversely, if the sediment volume deposited over a time period is greater than the flooding volume, then the system must undergo progradation. Through the creation of a sediment discharge model of the Mississippi River since the LGM, derived through the integration of a water discharge model of the Mississippi River since the LGM with a water flow velocity to sediment transport relationship of the modern Mississippi River, and the enumeration of the volumetric flooding volume, a model for both the timing and the magnitude the Mississippi River delta's progradation and retrogradation was created. From these models, it is predicted that Mississippi retrogradation did not begin until 16 ka, 2 ka after the LGM, due to a relatively low volumetric flooding rate as a result of basin morphological effects, leading to this interval having the highest volumetric rate of progradational magnitude in the post-LGM period. From this model, deltaic progradation is predicted to have resumed at ~8 ka, which is consistent with age dating of the Holocene-Pleistocene Surface. Distinct Holocene progradational events can be seen, which approximate the growth of different deltaic lobes.

Keywords: Modelling, Delta, Mississippi, Progradation, Last Glacial Maximum, Discharge, Flooding Volume

SHP
U

Aeolian Dune Height Controls on the Internal Architecture of Cross Sets: White Sands Dune Field, New Mexico

Xiafei Zhao
Zhao, X., The University of Texas at Austin
Cardenas, B., California Institute of Technology
Kim, W., Yonsei University

The stratal architecture in aeolian dunes contains a record of the transport and sorting of grains and are categorized into three primary dune stratifications: grainflow cross-strata, grainfall laminae, and wind ripple laminae. Previous studies are focused mainly on understanding slipface processes, leaving the relationship between aeolian stratal architecture and its formative dune unexplored. Here, we present field results from White Sands Dune Field, New Mexico, USA in order to understand how dune height controls the arrangement, abundance, and geometry of different stratification types. Grainflow thicknesses and widths were measured on wind-scoured stoss exposures for eight crescentic dunes with heights ranging from 1 m to 11 m. Dozens of grainflow thickness measurements were taken from successive horizontal exposures for each dune. The results showed that grainflow thickness averaged between 1 cm to 4 cm with no overall increasing trend between dune height and grainflow thickness. However, the tallest dune (11 m) produced many thick grainflow packages of 10 cm to 30 cm in which individual grainflows were indistinguishable and amalgamated. Thus, the amalgamation of bounding surfaces is characteristic of larger dunes due to the lack of grainfall separating the grainflows. Additionally, larger dunes typically produce wind ripple reworked bounding surfaces and stacked grainflows near the top of the dune and amalgamated contacts at the bottommost section where multiple grainflows merge in order to reach the base of a longer slipface. Smaller dunes were characterized by simple, lens-shaped grainflows separated by planar grainfall laminae. These measurements and stratigraphic differences will be useful in estimating original dune height in ancient cross-strata and will lead to a better interpretation of aeolian stratigraphy.

Keywords: aeolian, White Sands dune field, sediment, surface processes